Heat stress prevented the biomass and yield stimulation caused by elevated CO_2 in two well-watered wheat cultivars

Sachin G. Chavan[1], Remko A. Duursma[1], Michael Tausz[2], Oula Ghannoum[1]

[1]ARC Centre of Excellence for Translational Photosynthesis, Hawkesbury Institute for the Environment, Western Sydney University, Locked Bag 1797 Penrith NSW 2751 Australia.

[2]Institute for Future Farming Systems, Central Queensland University, Rockhampton QLD 4701 Australia

Corresponding author: Sachin Chavan, Email - S.Chavan@westernsydney.edu.au

Remko Duursma, Email - remkoduursma@gmail.com,

Michael Tausz, Email - m.tausz@cqu.edu.au

Oula Ghannoum, Email - O.Ghannoum@westernsydney.edu.au

Keywords: Wheat, elevated CO_2, photosynthetic acclimation, temperature response, heat stress, grain yield

Paper type: Primary research

Key message (<30 words)

High temperatures increased photosynthetic rates only at eCO_2 and photosynthesis was upregulated after recovery from heat stress at eCO_2 in Scout suggesting that eCO_2 increased optimum temperature of photosynthesis.

Abstract (250 words)

To investigate the interactive effects of elevated CO_2 and heat stress (HS), we grew two contrasting wheat cultivars, early-maturing Scout and high-tillering Yitpi, under non-limiting water and nutrients at ambient (aCO_2, 450 ppm) or elevated (eCO_2, 650 ppm) CO_2 and 22°C in the glasshouse. Plants were exposed to two 3-day HS cycles at the vegetative (38.1°C) and/or flowering (33.5°C) stage.

At aCO_2, both wheat cultivars showed similar responses of photosynthesis and mesophyll conductance to temperature and produced similar grain yield. Relative to aCO_2, eCO_2 enhanced photosynthesis rate and reduced stomatal conductance and maximal carboxylation rate (V_{cmax}). During HS, high temperature stimulated photosynthesis at eCO_2 in both cultivars, while eCO_2 stimulated photosynthesis in Scout. Electron transport rate (J_{max}) was unaffected by any treatment. eCO_2 equally enhanced biomass and grain yield of both cultivars in control, but not HS, plants. HS reduced biomass and yield of Scout at eCO_2. Yitpi, the cultivar with higher grain nitrogen, underwent a trade-off between grain yield and nitrogen. In conclusion, eCO_2 improved photosynthesis of control and HS wheat, and improved biomass and grain yield of control plants only. Under well-watered conditions, HS was not detrimental to photosynthesis or growth but precluded a yield response to eCO_2.

Key words: Wheat, photosynthesis, grain yield, elevated CO_2, heat stress, climate change

Introduction

Ongoing climate change is threatening the production of agricultural crops including wheat (*Triticum aestivum*) (Asseng *et al.*, 2015; Mishra *et al.*, 2021). By the end of this century, atmospheric carbon dioxide concentration ([CO_2]) is expected to reach 700 ppm, increasing surface temperatures by 1.1°C to 2.6°C (IPCC, 2014). For every degree of the temperature increase, global wheat production is predicted to decrease by 6–10% (Asseng *et al.*, 2015; García *et al.*, 2015). Crop models are important tools for assessing the impact of climate change (Asseng *et al.*, 2013). However, they largely lack the ability to consider genotype-specific responses to elevated [CO_2] (eCO_2) and their interaction with other environmental conditions. Hence, it is important to better understand how plants respond to eCO_2 interactions with the environment. Photosynthesis, a fundamental process driving crop growth and yield, can partially explain the interactive effects of eCO_2 with environmental stresses and provide a mechanistic basis for crop models (Yin and Struik, 2009).

During photosynthesis, ribulose-1, 5-bisphosphate carboxylase (Rubisco) catalyzes the carboxylation and oxygenation of ribulose-1, 5-bisphosphate (RuBP). eCO_2 increases photosynthetic rates (A_{sat}) and reduces photorespiration and stomatal conductance (g_s). Generally, higher photosynthetic rates enhance the growth and productivity of plants leading to increased leaf area, plant size and crop yield (Krenzer and Moss, 1975; Sionit *et al.*, 1981; Hocking and Meyer, 1991; Mitchell *et al.*, 1993; Kimball *et al.*, 1995; Mulholland *et al.*, 1998; Cardoso□Vilhena and Barnes, 2001; Högy *et al.*, 2009; Kimball, 2016; Fitzgerald *et al.*, 2016; Kimball, 1983). Following long term CO_2 enrichment, photosynthetic capacity may diminish due to lower amount of Rubisco (Nie *et al.*, 1995; Rogers and Humphries, 2000; Ainsworth *et al.*, 2003) or reduced activation of Rubisco (Delgado *et al.*, 1994).

Optimum temperature range for wheat growth is 17-23°C, with a minimum of 0°C and maximum of 37°C (Porter and Gawith, 1999). Global warming involves a gradual increase in mean temperature as well as increased frequency and intensity of heat waves. Heat can adversely affect crop growth and disrupt reproduction depending on the timing, intensity and duration (Sadras and Dreccer, 2015). Higher daytime temperatures (below damaging level) increase photosynthesis up to an optimum temperature, above which photosynthesis decreases mainly due to higher

72 photorespiration (Berry and Bjorkman, 1980; Long, 1991). High night time
73 temperatures increase respiration and reduce overall photosynthetic carbon gain
74 (Prasad *et al.*, 2008). At the whole plant level, high temperatures accelerate growth
75 (Fischer, 1980) and shorten crop duration (Hatfield and Prueger, 2015), hence
76 reducing grain yield due to insufficient time to capture resources. Losses due to short
77 crop duration are usually higher than benefits of growth stimulation at high
78 temperature (Wardlaw and Moncur, 1995).

79 The severity of the damage caused by abrupt temperature increases above the
80 optimum range (termed heat stress, HS) depends on the magnitude and duration of
81 HS as well as the developmental stage of the plant (Wahid et al., 2007). HS may
82 reduce photosynthesis due to reduced chlorophyll content, impaired photosystem II
83 and lower Rubisco activation (Berry and Bjorkman, 1980; Eckardt and Portis, 1997).
84 HS can directly damage cells and increase grain abortion resulting in reduced
85 growth, biomass and grain yield (Stone and Nicolas, 1996, 1998; Wardlaw *et al.*,
86 2002; Farooq *et al.*, 2011). Around anthesis, HS (>30°C) reduces seed setting due to
87 lower pollen viability, leading to poor fertilization, abnormal ovary development and
88 slower pollen growth (Balla *et al.*, 2019).

89 The interactive effects of eCO_2 and HS can be positive, negative or neutral (Wang et
90 al., 2008, 2011). Elevated CO_2 increases the temperature optimum of
91 photosynthesis (Long, 1991; Alonso *et al.*, 2009) by reducing photorespiration and
92 improving tolerance to photoinhibition (Hogan *et al.*, 1991). The impact of HS on
93 photosynthesis will depend on whether Rubisco, electron transport or end-product
94 synthesis is limiting at eCO_2 (Sage and Kubien, 2007). Enhanced growth and leaf
95 level water use efficiency (WUE) by eCO_2 may help compensate for the negative
96 impact of HS; conversely, heat-induced shortening of the grain-filling stage and grain
97 abortion could limit the benefits of eCO_2 (Lobell and Gourdji, 2012). In addition,
98 decreased g_s under eCO_2 may limit transpirational cooling and therefore exacerbate
99 HS. Thus, HS counteracts the positive effect of eCO_2 on yield components and may
100 aggravate the negative effect of eCO_2 on grain quality due to the high sensitivity of
101 wheat to temperature stress especially during anthesis and grain-filling stage (Wang
102 & Liu, 2021).

Many studies have investigated the response of wheat to eCO_2 in enclosures and in the field (Wang & Liu, 2021). However, only a few studies have considered eCO_2 interaction with temperature increases in wheat (Rawson, 1992; Delgado *et al.*, 1994; Morison and Lawlor, 1999; Jauregui *et al.*, 2015; Cai *et al.*, 2016) and rarely with HS (Coleman *et al.*, 1991; Wang *et al.*, 2008). Studies considering HS have addressed mainly the biomass or yield aspects and not the physiological processes such as photosynthesis (Stone and Nicolas, 1994, 1996, 1998). Interactive effects of eCO_2 and HS on photosynthesis have been reported in a limited number of studies (Wang *et al.*, 2008, 2011; Macabuhay, 2016; Macabuhay *et al.*, 2018; Chavan *et al.*, 2019). Macabuhay et al., (2018) studied interactive effects of eCO_2 and (experimentally imposed) heatwaves on wheat (cv Scout and Yitpi) grown in a dryland cropping system and concluded that eCO_2 may moderate some effects of HS on grain yield but such effects strongly depend on seasonal conditions and timing of HS. In another glasshouse experiment on the interactive effects of severe HS and eCO_2 in wheat (cv Scout), we found that eCO_2 mitigated the negative impacts of HS at anthesis on photosynthesis and biomass, but grain yield was reduced by HS in both CO_2 treatments (Chavan *et al.*, 2019). However, HS can occur throughout plant growth, including during vegetative, flowering or grain filling stages. In addition, different crop genotypes may respond variably to the interaction of eCO_2 with HS.

Here, we build on our previous work by comparing the interactive effects of eCO_2 and HS in two commercial wheat cultivars. Scout and Yitpi have similar genetic background but distinct agronomic features. Scout is a mid-season maturity cultivar with very good early vigor that can produce leaf area early in the season. Scout has a putative water-use efficiency (WUE) gene, which has been identified using carbon isotope discrimination (Condon *et al.*, 2004). Yitpi is a good early vigor, freely tillering, late flowering and long maturity cultivar (Bahrami et al., 2017; Pacificseeds, 2009; Seednet, 2005).

Although Scout is known to be a high yielding variety with very good grain quality and high reproductive sink (Pacific seeds, 2009), we hypothesized that Yitpi will produce higher grain yield due to its ability to initiate more tillers and its longer time to flower and mature (Hypothesis 1). Fast growing plants with high sink capacity show a greater eCO_2-induced growth stimulation (Poorter, 1993) and less

136 photosynthetic acclimation (Delgado *et al.*, 1994) compared to slow growing
137 counterparts with low sink capacity. Consequently, we hypothesized that Yitpi will
138 show greater photosynthetic, growth and yield response to eCO_2 due to its greater
139 vegetative sink capacity (tillering) relative to Scout with restricted tillering (Hypothesis
140 2). The greater growth stimulation at eCO_2 may buffer Yitpi against HS damage
141 compared to Scout. Thus, HS may decrease yield in Scout more than Yitpi and aCO_2
142 more than eCO_2 (Hypothesis 3). HS is more damaging at the reproductive relative to
143 the vegetative developmental stage (Farooq *et al.*, 2011). Hence, we expect less
144 damage in plants exposed to HS at the vegetative stage relative to the flowering
145 stage (Hypothesis 4).

146 To test these hypotheses, Scout and Yitpi were grown at ambient or elevated CO_2
147 conditions and subjected to one or two heat stresses at the vegetative (HS1) and/or
148 flowering (HS2) stage. Growth, biomass and photosynthetic parameters were
149 measured at different time points across the life cycle of the plants. At the plant level,
150 we report that eCO_2 equally stimulated grain yield of Scout and Yitpi. While
151 moderate HS under well-watered conditions was not detrimental to photosynthesis
152 and growth in the long term due to the transpirational cooling, HS prevented the
153 wheat plant from reaping the benefits of eCO_2 on biomass and yield.

Materials and methods

Plant culture and treatments

The experiment was conducted in the glasshouse facility located at the Hawkesbury campus of Western Sydney University (WSU). Seeds of commercial winter wheat cultivars Scout and Yitpi were procured from Agriculture Victoria (Horsham). Cultivars were selected based on their use in the Australian Grains Free Air CO_2 Enrichment (AGFACE) project investigating climate change impacts on wheat growth and yield (Houshmandfar *et al.*, 2017). For germination, 300 seeds of each cultivar were sterilized using 1.5 % $NaOCl_2$ for 1 min followed by incubation in the dark at 28°C for 48 hours in petri plates. Sprouted seeds were planted in germination trays using seed raising and cutting mix (Scotts, Osmocote®) at ambient CO_2 (aCO_2, 400 µl L^{-1}), temperature (22/14 °C day/night), relative humidity (RH, 50 to 70%) and natural light (midday average 500 µmol m^{-2} s^{-1}) (Figure S1). The growth stages are denoted by decimal code (DC) according to (Zadoks *et al.*, 1974) along with the time points here after. Two-week-old seedlings (DC12) were transplanted to individual cylindrical pots (15 cm diameter and 35 cm height) using sieved soil collected from local site. At transplanting stage (T0) pots were distributed into two aCO_2 (400 µl L^{-1}) and two eCO_2 (650 µl L^{-1}) chambers (Figure S1B). Some plants were exposed to one or two HS cycles at the vegetative (HS1, 10 weeks after planting, WAP, DC 32) and/or the flowering (HS2, 15 WAP, DC 63) stages for 3 days with temperature ramp up from 14°C night temperature (8 pm to 6 am) to 38°C during mid-day (10 pm to 4 pm) at 60% daytime RH (Figures S1 and S2). The two HS cycles created four sets of heat treatments at each CO_2 concentration as follows: (1) Control – plants were not exposed to HS at any stage, (2) HS1 – plants were exposed to HS at vegetative (DC32) stage only, (3) HS2 – plants were exposed to HS at reproductive (DC63) stage only and (4) HS1+2 – plants were exposed to both the heat stresses HS1 and HS2 (Figure S2).

Thrive all-purpose fertilizer (Yates) was applied monthly throughout the experiment to maintain similar nutrient supply in all treatment combinations. Pots were regularly swapped between left and right benches as well as between front and back for randomization within chamber. Pots and treatments were also swapped between the two ambient and two elevated CO_2 chambers for randomization among chambers.

Growth and biomass measurements

The full factorial experimental design included four chambers (two chambers for each CO_2 treatment) and five destructive harvests at time points T0 (2 WAP, DC12), T1 (6 WAP, DC28), T2 (10 WAP, DC35), T3 (17, DC65) and T4 (25 WAP, DC90) (Figure S2). Ten plants per treatment per cultivar were measured and harvested at each time point. Morphological parameters were measured followed by determinations of root, shoot and leaf dry mass. Samples were dried for 48 hours in the oven at 60°C immediately after harvesting. Leaf area was measured at time point T1, T2 and T3 using a leaf area meter (LI-3100A, LI-COR, Lincoln, NE, USA). Plant height, leaf number, tiller number and ear (grain inflorescence) number along with developmental stage information (booting (DC45), half-emerged (DC55) or fully emerged (DC60)) were recorded at time points T2 and T3).

Leaf gas exchange measurements

The youngest fully developed leaf (which was the flag leaf at T3) was used to measure gas exchange parameters. Instantaneous steady state leaf gas exchange measurements were performed at time points T1, T2 and T3 using a portable open gas exchange system (LI-6400XT, LI-COR, Lincoln, USA) to measure light-saturated (photosynthetic photon flux density (PPFD) =1500 µmol m^{-2} s^{-1}) photosynthetic rate (A_{sat}), stomatal conductance (g_s), ratio of intercellular to ambient CO_2 (C_i/C_a), leaf transpiration rate (E), dark respiration (R_d) and dark- and light-adapted chlorophyll fluorescence (Fv/Fm and Fv`/Fm`, respectively). Dark adapted leaf measurements were conducted by switching off light for 15 minutes. Steady state leaf gas exchange measurements were also performed during and after heat shock along with recovery stage. Plants were moved to a neighboring chamber with ambient CO_2 levels for short time (20-30 min for each plant) where air temperature was separately manipulated to achieve the desired leaf temperature. The LI-COR 6400-40 leaf chamber fluorometer (LCF) was used to measure gas exchange at a PPFD of 1500 µmol m^{-2} s^{-1} at two CO_2 concentrations (400 and 650 µl L^{-1}) and two leaf temperatures (25 and 35 °C). Photosynthetic down regulation or acclimation was examined by comparing the measurements at common CO_2 (ambient and elevated CO_2 grown plants measured at 400 µl L^{-1} CO_2 partial pressure) and growth CO_2

(aCO_2 grown plants measured at 400 µl L^{-1} CO_2 partial pressure and eCO_2 grown plants measured at 650 µl L^{-1} CO_2 partial pressure).

Dark respiration (R_d) was measured after a dark adaptation period of 15 minutes. Photosynthetic water use efficiency (PWUE) was calculated as A_{sat} (µmol m^{-2} s^{-1})/ g_s (mol m^{-2} s^{-1}). The response of A_{sat} to variations in sub-stomatal CO_2 mole fraction (*Ci*) (A-Ci response curve) was measured at T3 in 8 steps of CO_2 concentrations (50, 100, 230, 330, 420, 650, 1200 and 1800 µl L^{-1}) at leaf temperature of 25°C. Measurements were taken around mid-day (from 10 am to 3 pm) on attached last fully expanded or flag leaves of the main stems. Before each measurement, the leaf was allowed to stabilize for 10-20 minutes until it reached a steady state of CO_2 uptake and stomatal conductance. Ten replicate plants per treatment were measured.

Mesophyll conductance and temperature response

Mesophyll conductance (g_m) was determined by concurrent gas exchange and stable carbon isotope measurements using portable gas exchange system (LI-6400-XT, LI-COR, Lincoln, NE, USA) connected to a tunable diode laser (TDL) (TGA100, Campbell Scientific, Utah, USA) for the two wheat cultivars grown at ambient atmospheric CO_2 partial pressures. A_{sat} and $^{13}CO_2/^{12}CO_2$ carbon isotope discrimination were measured after T1 at five leaf temperatures (15, 20, 25, 30 and 35°C) and saturating light (1500 µmol quanta m^{-2} s^{-1}). Leaf temperature sequence started at 25°C decreasing to 15°C and then increased up to 35°C. Response of A_{sat} to variations in *Ci* was measured at each leaf temperature. Dark respiration was measured by switching light off for 20 minutes at the end of each temperature curve. Measurements were made inside a growth cabinet (Sanyo) to achieve desired leaf temperature. The photosynthetic carbon isotope discrimination (Δ) to determine g_m was measured as follows (Evans *et al.*, 1986)**:**

$$\Delta = \frac{1000\,\varepsilon(\delta^{13}C_{sam} - \delta^{13}C_{ref})}{1000 + \delta^{13}C_{sam} - \varepsilon(\delta^{13}C_{sam} - \delta^{13}C_{ref})} \quad (1)$$

$$\varepsilon = \frac{C_{ref}}{C_{ref} - C_{sam}} \quad (2)$$

Where,

C_{ref} and C_{sam} are the CO_2 concentrations of dry air entering and exiting the leaf chamber, respectively, measured by the TDl. g_m was calculated using correction for ternary and second-order effects (Farquhar and Cernusak, 2012; Evans and Von Caemmerer, 2013) following the next expression:

$$g_m = \frac{\frac{1+t}{1-t}\left(b - a_i - \frac{eR_d}{A+R_d}\right)\frac{A}{C_a}}{(\Delta_i - \Delta_o - \Delta_e - \Delta_f)} \quad (3)$$

Where, Δ_i is the fractionation that would occur if the *g*m were infinite in the absence of any respiratory fractionation (*e* = 0), Δ_o is observed fractionation, Δ_e and Δ_f are fractionation of ^{13}C due to respiration and photorespiration respectively (Evans and Von Caemmerer, 2013).

$$\Delta_i = \frac{1}{1-t}a'\frac{1}{(1-t)}((1+t)b - a')\frac{C_i}{C_a} \quad (4)$$

$$\Delta_e = \frac{1+t}{1-t}\left(\frac{eR_d}{(A+R_d)C_a}(C_i - \Gamma^*)\right) \quad (5)$$

$$\Delta_f = \frac{1+t}{1-t}\left(f\frac{\Gamma^*}{C_a}\right) \quad (6)$$

$$t = \frac{(1+a')E}{2g^t_{ac}} \quad (7)$$

Where,

The constants used in the model were as follows: E denotes transpiration rate; g^t_{ac} is total conductance to diffusion in the boundary layer (*a*b = 2.9‰) and in air (*a* = 4.4‰); *a*′ is the combined fractionation of CO_2 across boundary layer and stomata; net fractionation caused by RuBP and PEP carboxylation (*b* = 27.3‰) (Evans *et al.*, 1986); fractionation with respect to the average CO_2 composition associated with photorespiration (*f* = 11.6‰) (Lanigan *et al.*, 2008) and we assumed null fractionation associated with mitochondrial respiration in light (*e* = 0).

Leaf nitrogen and carbon estimation

Leaf discs were cut from the flag leaves used for gas exchange measurements at time points T2 and T3 then oven dried. Leaf discs were processed for nitrogen (N) and carbon (C) content using elemental analyzer (Dumas method). N and C were also estimated from other plant components including leaf, stem, root and grain

harvested at T1, T3 and T4. Ground samples were processed for C & N with a CHN analyzer (LECO TruMac CN-analyser, Leco corporation, USA) using an automated dry combustion method (Dumas method). Leaf N per unit area (N_{area}) was calculated as N (mmol g^{-1}) × LMA (g m^{-2}). Photosynthetic nitrogen use efficiency (PNUE) was calculated as A_{sat} (µmol m^{-2} s^{-1})/leaf N_{area} (mmol m^{-2}). Protein content was determined using N and multiplication factor of 5.7 (Mosse, 1990; Bahrami *et al.*, 2017).

Statistical and temperature analysis

All data analyses and plotting were performed using R computer software (R Core Team, 2020). The effect of treatments and their interactions was analyzed using linear modeling with 'anova' in R. Significance tests were performed with anova and post hoc Tukey test using the 'glht' function in the multcomp R package. Coefficient means were ranked using post-hoc Tukey test. The Farquhar-von Caemmerer-Berry (FvCB) photosynthesis model was fit to the A_{sat} response curves to C_i (A-Ci response curve) or chloroplastic CO_2 mole fraction (Cc), which was estimated from the g_m measurements (A-Cc response curve). We used the plantecophys R package (Duursma, 2015) to perform the fits, using measured g_m and R_d values, resulting in estimates of maximal carboxylation rate (V_{cmax}) and maximal electron transport rate (J_{max}) for D-ribulose-1,5-bisphosphate carboxylase/oxygenase (Rubisco) using measured R_d values. Temperature correction parameter (Tcorrect) was set to False while fitting A-C_i curves. Temperature response of V_{cmax} and J_{max} were calculated by Arrhenius and peaked functions, respectively (Medlyn *et al.*, 2002). Estimated V_{cmax} and J_{max} values at five leaf temperatures were then fit using nonlinear least square (nls) function in R to determine energy of activation for V_{cmax} (EaV) and J_{max} (EaJ) and entropy (ΔSJ). Temperature responses of V_{cmax} and R_d were fit using Arrhenius equation as follows,

$$f(Tk) = k_{25} \cdot exp\left[\frac{Ea \cdot (Tk - 298)}{R \cdot 298 \cdot Tk}\right] \quad (8)$$

Where, Ea is the activation energy (in J mol^{-1}) and k_{25} is the value of R_d or V_{cmax} at 25 °C. R is the universal gas constant (8.314 J mol^{-1} K^{-1}) and Tk is the leaf temperature in K. The activation energy term Ea describes the exponential rate of rise of enzyme activity with the increase in temperature. The temperature coefficient

Q_{10}, a measure of the rate of change of a biological or chemical system as a consequence of increasing the temperature by 10 °C was also determined for *Rd* using the following equation:

$$R_d = R_{d25} \cdot Q_{10}^{[(T-25)/10]} \quad (9)$$

A peaked function (Harley *et al.*, 1992) derived Arrhenius function was used to fit the temperature dependence of J_{max}, and is given by the following equation:

$$f(Tk) = k_{25} \cdot \exp\left[\frac{H_a \cdot (Tk - 298)}{R \cdot 298 \cdot Tk}\right] \left[\frac{1 + \exp\left(\frac{298 \cdot \Delta S - H_d}{298 \cdot R}\right)}{1 + \exp\left(\frac{Tk \cdot \Delta S - H_d}{Tk \cdot R}\right)}\right] \quad (10)$$

Where, Ea is the activation energy and k_{25} is the J_{max} value at 25 °C, Hd is the deactivation energy and S is the entropy term. Hd and ΔS together describe the rate of decrease in the function above the optimum. Hd was set to constant 200 kJ mol^{-1} to avoid over parametrization. The temperature optimum of J_{max} was derived from Eqn 10 (Medlyn *et al.*, 2002) and written as follows:

$$T_{opt} = \frac{H_d}{\Delta S - R \cdot \ln\left[\frac{E_a}{(H_d - E_a)}\right]} \quad (11)$$

The temperature response of A_{sat} was fit using a simple parabola equation (Crous *et al.*, 2013) to determine temperature optimum of photosynthesis:

$$A_{sat} = A_{opt} - b \cdot (T - T_{opt})^2 \quad (12)$$

Where, T is the leaf temperature of leaf gas exchange measurement for A_{sat}, T_{opt} represents the temperature optimum and A_{opt} is the corresponding A_{sat} at that temperature optimum. Steady state gas exchange parameters g_m, g_s, C_i and J_{max} to V_{cmax} ratio were fit using nls function with polynomial equation:

$$y = A + Bx + Cx^2 \quad (13)$$

Results

Two commercial wheat cultivars Scout and Yitpi were grown under aCO_2 or eCO_2 (daytime average of 450 or 650 µl L^{-1}, respectively; 65% RH and 22°C), natural sunlight and well-watered conditions (Figure S1). Both aCO_2 and eCO_2 grown plants were exposed to two 3-day HS cycles at the vegetative (HS1, 10 WAP, DC32, daytime average of 38°C) and flowering stage (HS2, 15 WAP, DC63, daytime average of 33.5°C), while daytime RH was maintained at 60%. HS2 was lower in intensity relative to HS1 due to the cool winter conditions. Both HS cycles had similar overall effects on growth and yield parameters, refuting our fourth hypothesis that HS during the reproductive stage is more damaging. Hence, we mostly compare the control plants to those exposed to both heat stresses. Grain filling started 17 WAP (DC65) and final harvest occurred 25 WAP (DC90) (Figure S2).

Photosynthetic temperature responses of the two wheat cultivars at aCO_2

A-C_i curves together with g_m were measured at five leaf temperatures to characterize the thermal photosynthetic responses of the two wheat cultivars grown at aCO_2 (Figure 1; Table 1). Overall, both cultivars had similar photosynthetic temperature responses. A_{sat} and g_s increased with leaf temperature up to an optimum (T_{opt}) around 23.4°C and decreased thereafter, while C_i slowly decreased with temperature. Mesophyll conductance (g_m) increased up to 25°C then plateaued (Figure 1B). The temperature response of g_m as well as the values recorded at 25°C (0.25-0.31 mol m^{-2} s^{-1} bar^{-1}) for Scout and Yitpi (Figure 1B) were similar to what has been reported for wheat (0.39) and other crop species (cotton = 0.73, soybean = 0.49 and rice = 0.67) (Von Caemmerer and Evans, 2015; Jahan *et al.*, 2021). Scout had slightly higher A_{sat}, g_s and g_m than Yitpi at most leaf temperatures (Figures 1A-D). R_d linearly increased with temperature, and both cultivars had similar Q_{10} (Figure 1H, Table 1). V_{cmax} and J_{max} exponentially increased with leaf temperature, but J_{max} declined above T_{opt} (30°C) in both cultivars (Figures 1E-F). There was no significant difference in V_{cmax}, J_{max} or their activation energies between the two wheat cultivars (Figure 1E-G, Table 1). The ratio of J_{max}/V_{cmax} was similar for the two cultivars and linearly decreased with leaf temperature (Figure 1G).

eCO$_2$ stimulated photosynthesis and reduced stomatal conductance in both wheat cultivars

Overall, the two wheat cultivars had similar A_{sat}, g_s, PWUE (A_{sat}/g_s), R_d, Fv/Fm, V_{cmax} and J_{max} measured under most conditions (Figures 1-4, Tables S1-S3). Under control (non-HS) conditions, eCO$_2$ enhanced A_{sat} measured at growth CO$_2$ (A_{growth}) and 25℃ and reduced g_s in both cultivars at T1, T2 and T3 (Figure 2, Tables S1-S3). When measured at common CO$_2$ and 25^{o}C, eCO$_2$-grown plants had lower A_{sat} (-12% at T2, p <0.01) and g_s (-10% at T2, p <0.001) relative to aCO$_2$. This photosynthetic downregulation was more persistent in Yitpi compared to Scout (Figure 2, Tables S1-S3).

High temperature during HS enhanced photosynthesis under eCO$_2$

The two HS cycles did not reduce A_{growth} measured at 25℃ during or after HS (Figure 3A-D, Tables S1-S3). During both HS1 and HS2, eCO$_2$ stimulated A_{growth} measured at 25℃ in Scout but not Yitpi. Relative to 25°C, A_{growth} increased at 35°C in Scout (10-14%) and Yitpi (12-18%) grown at eCO$_2$ but not at aCO$_2$. Immediately after the recovery from HS, A_{growth} was upregulated in eCO$_2$-grown Scout (Figures 3A-D and S3). During both HS cycles, dark-adapted Fv/Fm measured at 25℃ tended to be lower in Yitpi grown at eCO$_2$ relative to aCO$_2$. In both cultivars, Fv/Fm decreased at 35℃ relative to 25^{o}C, indicating transient damage to PSII due to HS at both CO$_2$ treatments (Figure 3E-H, Tables S1-S3).

Following long-term recovery from HS1 and/or HS2, the eCO$_2$ stimulation of A_{growth} was still marginally apparent in all T3 plants, being the strongest in eCO$_2$-grown Yitpi (Figure 4A-B, Tables S1-S3). The reduction of g_s at eCO$_2$ was weak in all plants (Figure 4C-D, Tables S1-S3). Hence, PWUE was stimulated by eCO$_2$ in all treatments, while PNUE was unaffected (Figure 4E-H, Tables S1-S3). There was a good correlation between A_{growth} and g_s (r^2 = 0.51, p <0.001) across all treatments (Figure 5A).

V_{cmax} and J_{max} were derived from A-C$_i$ response curves measured at 25°C during the recovery stage after HS2. For control and HS plants, growth at eCO$_2$ marginally reduced V_{cmax} in Scout (-14%, p = 0.09) and Yitpi (-15%, p = 0.06) but had no effect on J_{max}. HS had no effect on V_{cmax} or J_{max} in either cultivar (Figure 4I-L, Tables S1-

S3). V_{cmax} and J_{max} correlated well (r^2 = 0.75, p <0.001) across treatments (Figure 5B).

Yitpi produced more tillers and grains than Scout

When compared at aCO_2, the two wheat cultivars differed in phenology and growth habit. Scout developed faster and flowered earlier than Yitpi. At T2, 43% of tillers had ears in Scout compared to 11% in Yitpi (Figure S4). At T2, Scout was 74% (p < 0.001) taller than Yitpi but at T3 both cultivars had similar height (Figure 6I-J, Tables S4 and S5). In contrast, Yitpi accumulated more biomass relative to Scout by producing more tillers. At T3, Yitpi had 42% (p < 0.005) more total plant biomass, 130% (p < 0.001) more tillers, 254% (p < 0.001) larger leaf area, 128% (p < 0.001) more leaves and 61% (p < 0.001) larger leaf size compared to Scout (Figure 6, Tables S4 and S5).

At the final harvest (T4), Yitpi had more plant biomass (84%, p < 0.001), tillers (88%, p < 0.001) and number of grains (54%, p < 0.001). Conversely, Scout had larger grain size (+31%, p < 0.001), a higher proportion (100%) of its tillers developed ears and more ears filled grains compared to higher tillering Yitpi (88%). Hence, both cultivars had relatively similar grain yield (g/plant) (Figure 7A-F, Tables S4 and S6). Higher (178%, p < 0.001) harvest index (HI) in Scout was due to early maturity and consequent leaf senescence leading to loss of biomass at final harvest (Tables S5). The final harvest was undertaken four weeks after all ears had matured on Scout to give ample time for grain filling in Yitpi (Figure 7, Tables S4 and S6).

eCO_2 similarly stimulated wheat biomass and grain yield under non-HS conditions

The increase in plant biomass at eCO_2 depended on the growth stage (Figures 6-7, Tables S4 and S5). However, the overall stimulation was not different between the two cultivars as evident from the non-significant eCO_2 x cultivar interaction at all harvests (Table S4). By T3 (anthesis), when both cultivars were still within the exponential growth stage, eCO_2 stimulated plant biomass of Yitpi (+29%, p < 0.001) and Scout (+9%, p < 0.001) under control conditions. The number of tillers, total leaf area, mean leaf size or leaf mass area were not significantly affected by eCO_2 in either cultivar (Figure 6, Tables S4 and S5). eCO_2 increased allocation to stem

relative to leaf biomass, particularly in Yitpi. Accordingly, there was a strong correlation across treatments between stem and leaf biomass (r^2 = *0.83*, p < 0.001) and between total biomass and leaf area (r^2 = *0.83*, p < 0.001) in Scout but not in Yitpi. However, the two cultivars followed common relationship for root *versus* shoot biomass (r^2 = *0.41,* p < 0.001) and leaf area *versus* leaf number (r^2 = *0.82*, p < 0.001) across all treatments suggesting no effect of cultivar, eCO_2 or HS on these common allometric relationships (Figure S5, Table S5).

At the final harvest T4 (seed maturity), eCO_2 enhanced biomass and equally stimulated grain yield by increasing grain number in both cultivars (+64% in Scout and +50% in Yitpi) under control conditions only (Figure 7A-D, Tables S4-S6). Harvest index was not directly affected by any treatments but showed a significant interaction (p <0.05) between CO_2 and cultivar, such that HI was higher in Yitpi under eCO_2 (Tables S5 and S6).

eCO₂ did not stimulate the grain yield of HS plants

At T3, moderate HS (34-38°C) applied under well-watered conditions and 60% RH during the vegetative (HS1 applied after T1) and flowering (HS2 applied after T2) stages had no significant impact on plant biomass of either wheat cultivar or CO_2 treatment. By T4, there were significant HS x CO_2 x cultivar interactions (p < 0.01) for biomass and grain yield. HS1+2 reduced the biomass and grain yield of eCO_2-grown Scout relative to aCO_2-grown counterparts. Unlike control plants, the biomass and yield of HS plants were not enhanced by eCO_2 (Figure 7, Tables S4 and S5).

eCO₂ reduced grain N in Yitpi **but not in Scout**

Neither eCO_2 or HS had a significant effect on flag leaf N content in either cultivar at T2 or T3, but eCO_2 reduced aggregate leaf N content (-18%) at T3 in Yitpi only (Cultivar x CO_2 p < 0.05) (Table S7). Yitpi had higher grain N content (+26%) than Scout in control plants grown at aCO_2 (Figure 7G-H, Table S6). In control plants, eCO_2 significantly reduced grain protein content in Yitpi (-18%, p < 0.05) but not in Scout due to significant cultivar X CO_2 interaction (p < 0.01), while HS had no effect on protein content in either cultivar (Figure 7G-H, Table S6).

Discussion

Two wheat cultivars with contrasting morphology and phenology, but similar photosynthesis and grain yield

The effects of future climate conditions, including eCO_2, will depend on the environmental conditions (e.g., water and heat stress) and the crop's agronomic features. Here, we compared the interactive effects of eCO_2 and HS on two commercial wheat cultivars, Scout and Yitpi, with contrasting phenology and growth habit. Plants were grown under well-watered and fertilized conditions to remove any confounding effects of water or nutrient limitations on the eCO_2 or HS responses. RH was kept constant to minimize the negative impact of dry air during HS. Finally, we compared the effects of applying HS at the vegetative and flowering stages.

Free tillering Yitpi produced substantially more tillers, leaf area and biomass relative to the faster developing Scout. Accordingly, our first hypothesis predicted that Yitpi will have higher grain yield. The results only partially supported this hypothesis, because relative to Yitpi, Scout had higher harvest index (HI) due to its early maturing and senescing habit. While Yitpi initiated more tillers, a lower proportion of these tillers produced ears and filled grains. In contrast, Scout produced less tillers but flowered earlier which allowed enough time for all its tillers to produce ears and fill bigger grains by the final harvest. Hence, both cultivars had relatively similar yields due to bigger grain size in Scout and higher grain number in Yitpi. It is worth noting that some field trials have reported slightly higher grain yields in Scout than Yitpi (National variety trial report, GRDC, 2014). Our results are consistent with a previous study using different wheat cultivars with contrasting source-sink relationships which reported that the freely tillering cultivar "Silverstar" translated into more spikes while restricted tillering cultivar "H45" had more and heavier kernels per spike than "Silverstar" (Tausz-Posch et al., 2015). Thus, early vigor and maturity compared to high tillering capacity seem to be equally beneficial traits for high grain yield in the Australian environment.

The two wheat cultivars showed similar photosynthetic traits and response to temperature and eCO_2. In contrast to our expectations that Scout would have higher WUE due to its selection based on a carbon isotope discrimination gene (Condon *et*

al., 2004), both wheat cultivars showed similar PWUE under most measurement and growth conditions in this study (Figure 4E-F, Table 2).

Elevated CO_2 stimulated photosynthesis but reduced photosynthetic capacity in both cultivars

Long term exposure to eCO_2 may reduce photosynthetic capacity due to lower amount of Rubisco in a process referred as 'acclimation' (Nie *et al.*, 1995; Rogers and Humphries, 2000; Ainsworth *et al.*, 2003). Alternatively, eCO_2 may 'down-regulate' photosynthetic capacity by reducing Rubisco activation or other regulatory mechanisms without affecting Rubisco content (Delgado *et al.*, 1994). In the current study, eCO_2 similarly increased A_{growth} (+21%) measured at growth CO_2 and reduced both A_{sat} (-12%) measured at common CO_2 (Figure 2, T2) and V_{cmax} (Figure 4I-J) in both cultivars. In contrast, leaf N (and possibly Rubisco) was not significantly affected in either cultivar (Table S4). Hence, the wheat cultivars have likely undergone a photosynthetic downregulation -rather than acclimation- in response to eCO_2 (Delgado *et al.*, 1994; Leakey *et al.*, 2009). These results partially countered our second hypothesis suggesting that Yitpi will show less photosynthetic acclimation due to its higher sink capacity. The interaction of eCO_2 with plant traits are complex. On the one hand, eCO_2 is expected to cause less feedback inhibition on photosynthesis in plants with high sink capacity (Ainsworth *et al.*, 2004). On the other, fast-growing plants show a proportionally larger response to eCO_2 (Poorter and Navas, 2003). Hence, high tillering in Yitpi and fast development in Scout both led to a relatively small observed photosynthetic downregulation in response to growth at eCO_2. This allowed a sustained photosynthetic stimulation, which in turn led to a significant biomass and yield enhancement by CO_2 enrichment in both wheat cultivars (Figures 6-7). Photosynthetic responses of wheat in current study are in agreement with earlier enclosure studies which generally have higher response to eCO_2 than the FACE studies (Kimball *et al.*, 1995; Hunsaker *et al.*, 1996; Osborne *et al.*, 1998; Kimball *et al.*, 1999; Long *et al.*, 2006; Cai *et al.*, 2016).

Elevated CO_2 stimulated grain yield similarly in both wheat cultivars

In disagreement with our second hypothesis, eCO_2 similarly stimulated plant biomass and grain yield in early-maturing Scout and high tillering Yitpi (Figures 6-7, Table S4-S5). In Scout, the biomass stimulation was associated with increased

tillering (one extra tiller per plant). In contrast, Yitpi produced many tillers at aCO_2 and the additional fixed carbon at eCO_2 was allocated to the existing tillers. At seed maturity, eCO_2 stimulated grain yield similarly in both cultivars as a result of the trade-off between grain yield components (Dias de Oliveira *et al.*, 2015). In particular, eCO_2 stimulated grain number in both cultivars, while grain size increased in Scout only (Figure 7, Table S6). Generally, eCO_2 stimulates grain yield by increasing the number of tillers and consequently, ears per plant (Zhang *et al.*, 2010; Bennett *et al.*, 2012), which has also been reported in FACE studies (Högy *et al.*, 2009; Tausz-Posch *et al.*, 2015; Fitzgerald *et al.*, 2016). However, in our study, the increase in grain yield at eCO_2 was mainly due to the increase in the number of grains per ear. In line with our results, Tausz-Posch et al., (2015) reported comparable grain yield stimulation by eCO_2 in two different wheat cultivars with contrasting source-sink relationships. Moreover, grain yield of twenty wheat cultivars that differed in tillering propensity, water soluble carbohydrate accumulation, early vigor and transpiration efficiency responded similarly to eCO_2 in glasshouse settings (Ziska *et al.*, 2004; Bourgault *et al.*, 2013).

Elevated CO_2 reduced grain N in Yitpi only

Overall, there is a negative relationship between grain yield and quality (Taub *et al.*, 2008; Pleijel and Uddling, 2012). Hence, increased grain yield at eCO_2 results in lower grain N and hence protein content (Seneweera and Conroy, 1997; Bahrami *et al.*, 2017). In our study, eCO_2 reduced grain N in Yitpi under control conditions. Scout was characterized by having larger grains which accumulated less N than Yitpi. Moreover, eCO_2 reduced total leaf N (-18%) at T3 and grain N (-17 %) at T4 in Yitpi but not in Scout. This is consistent with the results from FACE study with same cultivars which reported -14% reduction in N content by eCO_2 in above ground dry mass in Yitpi but not in Scout under well-watered conditions (Bahrami *et al.*, 2017). The higher biomass accumulation in free tillering Yitpi may have exhausted the nutrient supply, such that further biomass stimulation by eCO_2 lead to a significant dilution in N content (Taub and Wang, 2008).

Wheat cultivars with early vigour such as Scout have greater root biomass accumulation as well as greater early N uptake which may have avoided a negative effect of eCO_2 on leaf and grain N (Liao *et al.*, 2004; Bahrami *et al.*, 2017).

Accordingly, Scout maintained a higher N utilization efficiency (grain yield per total plant N) relative to Yitpi under all treatments (Table S6). Increased grain yield is strongly associated with higher grain number per unit area (Zhang *et al.*, 2010; Bennett *et al.*, 2012) which dilutes the amount of N translocated per grain. Quality deterioration due to lower protein via reduced N is of critical concern in future high CO_2 climate considering that even additional supply of N does not prevent N dilution in grain under eCO_2 (Tausz *et al.*, 2017). In addition, eCO_2 has strong detrimental effect on other nutrient availability and remobilization from leaves to grains (Tcherkez *et al.*, 2020).

HS had little effects on wheat photosynthesis or yield at aCO_2

A key finding of this study was that the application of HS events (HS1, HS2 or HS1+2) was not detrimental to aCO_2-grown wheat plants (Figures 5 and 7, Tables S4-S6). Thus, our hypothesis that HS will reduce photosynthesis, biomass and yield at aCO_2 was rejected. This finding is in contrast to previously reported studies where HS reduced the grain yield and negatively affected the growth and development in wheat (Stone and Nicolas, 1996, 1998; Farooq et al., 2011; Coleman et al., 1991). During heat waves in the field, the vapor pressure deficit (VPD) increases and soil moisture decreases leading to lower stomatal conductance and consequently lower transpiration rate. Thus, plants are unable to cool down and leaf temperatures rise beyond optimum levels causing damage. The negligible effect of HS in our study could be explained by the ability of well-watered plants to maintain leaf temperature below damaging levels due to transpirational cooling (Perera *et al.*, 2019; Deva *et al.*, 2020) even with air temperatures reaching up to 38°C. At moderate (~60%) relative humidity, there is sufficient water vapour gradient to sustain high transpiration rates when soil water is available, as was the case in our experiment. In most cases, g_s was not significantly affected (Tables S1 and S2), and even slightly higher at T3 in HS-pants relative to the control (Figure 4c,d) Well-watered crops can maintain grain-filling rate, duration and size under HS (Dupont *et al.*, 2006), and high temperatures can increase crop yields if not exceeding critical optimum growth temperature (Welch *et al.*, 2010). Also, in the current study, the night temperatures were not increased during HS which favors plant growth by reducing respiratory losses (Prasad *et al.*, 2008).

In particular, HS did not elicit a direct negative impact on photosynthesis or chlorophyll fluorescence in either cultivar or CO_2 treatment. During HS, high temperature transiently reduced maximum efficiency of PSII (Fv/Fm) in both cultivars and CO_2 treatments (Figure 3E-H). However, unchanged Fv/Fm measured at 25^{o}C confirmed that photosynthesis did not suffer long-term damage during or after HS. Moreover, HS was not severe enough to negatively affect A_{growth} measured at 25°C. These results are corroborated by the insensitivity of V_{cmax} and J_{max} to HS (Figure 4I-L), but contrast with previously reported studies where HS reduced photosynthesis in wheat at the vegetative (Wang et al., 2008) and the flowering (Chavan *et al.*, 2019; Balla *et al.*, 2019) stages. HS lowers membrane thermostability by inducing reactive oxygen species (ROS) and altering the membrane protein structures, which lead to changes in the fluidity of the thylakoid membrane and separation of light harvesting complex from the photosystems (Wahid *et al.*, 2007; Poudel, 2020). We were unable to measure leaf temperatures in the current study, but we speculate that, in well-watered wheat plants growing at moderate RH, leaf temperatures might not have increased beyond damaging levels to the membranes during the HS events.

Repeated HS may result in priming which involves pre-exposure of plants to a stimulating factor such as HS (Wang *et al.*, 2017) and enable plants to cope better with later HS events (Balla *et al.*, 2021). However, there was no difference between HS applied at the vegetative (HS1) and/or flowering stage (HS2) in rejection of our fourth hypothesis, and this may additionally be due to the short term duration of the two HS cycles (3 days each). Hence, our study demonstrated the benign effect that HS has on crop yield when separated from water stress and plants are able to transpire.

HS precluded an eCO_2 response in biomass and grain yield

In our study, the impact of HS depended on the wheat cultivar and growth CO_2 (Tables S1 and S4). Elevated CO_2 and temperature interactions can be complex, dynamic and difficult to generalize as they can go in any direction depending on plant traits and other environmental conditions (Rawson, 1992). Plant development is generally accelerated by increased temperature; eCO_2 can accelerate it further in some instances or may have neutral or even retarding effects in other cases (Rawson, 1992).

While eCO_2 stimulated wheat biomass and grain yield under control (non-HS) conditions, HS precluded a yield response to eCO_2 in Yitpi and reduced biomass and yield in eCO_2-grown Scout relative to aCO_2-grown counterparts (Figure 7). These results are in contrast with previous studies that reported similar wheat yield reduction at ambient or elevated CO_2 in response to severe (Chavan *et al.*, 2019) or moderate HS (Zhang *et al.*, 2018). The results also partially refuted our third hypothesis that HS may decrease yield more at aCO_2 than eCO_2, while partially agreeing that HS will have a more negative impact on Scout relative to Yitpi, albeit for different reasons than what we originally suggested. The negative effect of HS on Scout biomass and grain yield at eCO_2 occurred despite the eCO_2 stimulation of A_{growth} under HS (T3, Figure 4). However, over the long term, A_{growth} was stimulated in eCO_2-grown Yitpi and not Scout (Figure 4).

Lack of a biomass stimulation despite high photosynthetic rates during HS under eCO_2 could be due to the short duration of HS (3 days), which may not have been long enough to stimulate biomass gain. In addition, nutrient limitation at eCO_2 may have restricted the eCO_2 growth response. Typically, eCO_2 studies show reduced N content in wheat and other crops (Taub and Wang, 2008; Leakey *et al.*, 2009; Bahrami *et al.*, 2017). Hence, the wheat plants may have exhausted available nutrients due to increased demand by growing sinks at eCO_2, which may limited further stimulation by high temperature. HS may be more damaging at eCO_2 due to reduce transpirational cooling as a result of reduced g_s at eCO_2, leading to higher leaf temperatures. However, A_{growth} increased in response to high temperature (35°C) under eCO_2 but not under aCO_2 during HS (Figure 3A-D), which refutes the suggestion of HS-damage to photosynthesis.

Higher g_s during HS at moderate RH in well-watered conditions may increase A_{growth} by increasing C_i in both aCO_2 and eCO_2 grown plants. Furthermore, lower photorespiration under eCO_2 allows additional increase in A_{growth} with temperature when measured at 35°C relative to 25°C (Long, 1991). Under aCO_2, photorespiration increases with temperature reducing A_{growth} measured at 35°C relative to 25°C. Our results also point to a shift in T_{opt} of photosynthesis (~ 24°C at aCO_2) to higher temperatures for plants grown at eCO_2 (Sage and Kubien, 2007). This would come about as a result of lower photorespiration at eCO_2 as well as the slight upregulation of photosynthetic rates observed in eCO_2-grown Scout at the recovery stage of HS

(Figure 3A, C). However, at T3, A_{growth} was similar between aCO_2 and eCO_2 grown plants (Figure 4A) indicating the short-term nature of this photosynthetic upregulation.

Conclusions

The two wheat cultivars, Scout and Yitpi differed in growth and development but produced similar grain yield. Under control conditions, eCO_2 stimulated biomass and yield similarly in both cultivars. HS was not damaging to photosynthesis, growth, biomass or grain yield under well-watered and moderate RH conditions. However, HS interacted with eCO_2, leading to similar or lower biomass and grain yield at eCO_2 relative to both aCO_2 in plants exposed to HS. This interactive effect precluded the positive effects of eCO_2 in HS-plants. eCO_2 improved photosynthetic rates in control and HS plants. Also, high temperature stimulated photosynthesis under eCO_2 but not under aCO_2 during HS which suggests increased optimum temperature of photosynthesis at eCO_2. We speculate that in the current study, HS plants were able to cool down using high transpiration which helped to maintain lower leaf temperatures despite high air temperatures during HS. The current study provides important insights into the effect of short-term moderate temperature increases in well-watered conditions under future elevated CO_2, potential role of transpirational cooling during HS and interactions between HS and eCO_2 which will be useful in breeding cultivars for future climate and improving crop model accuracy to predict crop performance in future high CO_2 environment with frequent heat waves.

Acknowledgments

We gratefully acknowledge the technical support of Fiona Koller. SGC was supported by the 'Agriculture, Fisheries & Forestry Postgraduate Research Scholarship' and Western Sydney University. The research received funding support by the Australian Commonwealth Department for Agriculture and Water Resources through the 'Filling the research gap' programme and was associated with the Australian Grains Free Air CO_2 Enrichment (AGFACE) programme run jointly by The University of Melbourne and Agriculture Victoria. OG was also funded by the Australian Research Council Centre of Excellence for Translational Photosynthesis (CE140100015).

Conflicts of interest

The authors declare that they have no conflict of interest.

Availability of data

All data supporting the findings of this study are available within the paper and within its supplementary materials published online. Reuse of the data is permitted after obtaining permission from the corresponding author.

Code availability

Software application and codes used are all publicly available.

Authors contributions

All authors conceived the project. SGC maintained the plants and collected the data. SGC and RAD analysed the data. SGC and OG prepared the manuscript with input from other co-authors.

References

Ainsworth EA, Davey PA, Hymus GJ, Osborne CP, Rogers A, Blum H, Nösberger J, Long SP. 2003. Is stimulation of leaf photosynthesis by elevated carbon dioxide concentration maintained in the long term? A test with Lolium perenne grown for 10 years at two nitrogen fertilization levels under Free Air CO2Enrichment (FACE). Plant, Cell & Environment **26**, 705–714.

Ainsworth EA, Rogers A, Nelson R, Long SP. 2004. Testing the "source–sink" hypothesis of down-regulation of photosynthesis in elevated [CO2] in the field with single gene substitutions in Glycine max. Agricultural and Forest Meteorology **122**, 85–94.

Alonso A, Pérez P, Martínez-Carrasco R. 2009. Growth in elevated CO2 enhances temperature response of photosynthesis in wheat. Physiologia Plantarum **135**, 109–120.

Asseng S, Ewert F, Martre P, *et al.* 2015. Rising temperatures reduce global wheat production. Nature Climate Change **5**, 143–147.

Asseng S, Ewert F, Rosenzweig C, *et al.* 2013. Uncertainty in simulating wheat yields under climate change. Nature Climate Change **3**, 827–832.

Bahrami H, De Kok LJ, Armstrong R, Fitzgerald GJ, Bourgault M, Henty S, Tausz M, Tausz-Posch S. 2017. The proportion of nitrate in leaf nitrogen, but not changes in root growth, are associated with decreased grain protein in wheat under elevated [CO2]. Journal of Plant Physiology **216**, 44–51.

Balla K, Karsai I, Bónis P, Kiss T, Berki Z, Horváth Á, Mayer M, Bencze S, Veisz O. 2019. Heat stress responses in a large set of winter wheat cultivars (Triticum aestivum L.) depend on the timing and duration of stress. PLoS ONE **14**, e0222639.

Balla K, Karsai I, Kiss T, Horváth Á, Berki Z, Cseh A, Bónis P, Árendás T, Veisz O. 2021. Single versus repeated heat stress in wheat: What are the consequences in different developmental phases? PLOS ONE **16**, e0252070.

Bennett D, Izanloo A, Reynolds M, Kuchel H, Langridge P, Schnurbusch T. 2012. Genetic dissection of grain yield and physical grain quality in bread wheat (Triticum aestivum L.) under water-limited environments. Theoretical and Applied Genetics **125**, 255–271.

Berry J, Bjorkman O. 1980. Photosynthetic Response and Adaptation to Temperature in Higher Plants. Annual Review of Plant Physiology **31**, 491–543.

Bourgault M, Dreccer MF, James AT, Chapman SC. 2013. Genotypic variability in the response to elevated CO2 of wheat lines differing in adaptive traits. Functional Plant Biology **40**, 172–184.

Cai C, Yin X, He S, *et al.* 2016. Responses of wheat and rice to factorial combinations of ambient and elevated CO2 and temperature in FACE experiments. Global Change Biology **22**, 856–874.

Cardoso-Vilhena J, Barnes J. 2001. Does nitrogen supply affect the response of wheat (Triticum aestivum cv. Hanno) to the combination of elevated CO2 and O3? Journal of Experimental Botany **52**, 1901–1911.

Chavan SG, Duursma RA, Tausz M, Ghannoum O. 2019. Elevated CO2 alleviates the negative impact of heat stress on wheat physiology but not on grain yield. Journal of Experimental Botany.

Coleman JS, Rochefort L, Bazzaz FA, Woodward FI. 1991. Atmospheric CO2, plant nitrogen status and the susceptibility of plants to an acute increase in temperature. Plant, Cell & Environment **14**, 667–674.

Condon AG, Richards RA, Rebetzke GJ, Farquhar GD. 2004. Breeding for high water-use efficiency. Journal of Experimental Botany **55**, 2447–2460.

Crous KY, Quentin AG, Lin Y-S, Medlyn BE, Williams DG, Barton CVM, Ellsworth DS. 2013. Photosynthesis of temperate Eucalyptus globulus trees outside their native range has limited adjustment to elevated CO2 and climate warming. Global Change Biology **19**, 3790–3807.

Delgado E, Mitchell R a. C, Parry M a. J, Driscoll SP, Mitchell VJ, Lawlor DW. 1994. Interacting effects of CO2 concentration, temperature and nitrogen supply on the photosynthesis and composition of winter wheat leaves. Plant, Cell & Environment **17**, 1205–1213.

Deva CR, Urban MO, Challinor AJ, Falloon P, Svitákova L. 2020. Enhanced Leaf Cooling Is a Pathway to Heat Tolerance in Common Bean. Frontiers in Plant Science **11**, 19.

Dias de Oliveira EA, Siddique KHM, Bramley H, Stefanova K, Palta JA. 2015. Response of wheat restricted-tillering and vigorous growth traits to variables of climate change. Global Change Biology **21**, 857–873.

Dupont FM, Hurkman WJ, Vensel WH, Tanaka C, Kothari KM, Chung OK, Altenbach SB. 2006. Protein accumulation and composition in wheat grains: Effects of mineral nutrients and high temperature. European Journal of Agronomy **25**, 96–107.

Duursma RA. 2015. Plantecophys - An R Package for Analysing and Modelling Leaf Gas Exchange Data. PLoS ONE **10**, e0143346.

Eckardt NA, Portis AR. 1997. Heat Denaturation Profiles of Ribulose-1,5-Bisphosphate Carboxylase/Oxygenase (Rubisco) and Rubisco Activase and the Inability of Rubisco Activase to Restore Activity of Heat-Denatured Rubisco. Plant Physiology **113**, 243–248.

Evans J, Sharkey T, Berry J, Farquhar G. 1986. Carbon Isotope Discrimination measured Concurrently with Gas Exchange to Investigate CO2 Diffusion in Leaves of Higher Plants. Functional Plant Biology **13**, 281–292.

Evans J, Von Caemmerer S. 2013. Temperature response of carbon isotope discrimination and mesophyll conductance in tobacco. Plant, Cell & Environment **36**, 745–756.

Farooq M, Bramley H, Palta JA, Siddique KHM. 2011. Heat Stress in Wheat during Reproductive and Grain-Filling Phases. Critical Reviews in Plant Sciences **30**, 491–507.

Farquhar GD, Cernusak LA. 2012. Ternary effects on the gas exchange of isotopologues of carbon dioxide. Plant, Cell & Environment **35**, 1221–1231.

Fischer RA. 1980. Influence of water stress on crop yield in semiarid regions. Influence of water stress on crop yield in semiarid regions.

Fitzgerald GJ, Tausz M, O'Leary G, *et al.* 2016. Elevated atmospheric [CO2] can dramatically increase wheat yields in semi-arid environments and buffer against heat waves. Global Change Biology **22**, 2269–2284.

García GA, Dreccer MF, Miralles DJ, Serrago RA. 2015. High night temperatures during grain number determination reduce wheat and barley grain yield: a field study. Global Change Biology **21**, 4153–4164.

Harley PC, Thomas RB, Reynolds JF, Strain BR. 1992. Modelling photosynthesis of cotton grown in elevated CO2. Plant, Cell & Environment **15**, 271–282.

Hatfield JL, Prueger JH. 2015. Temperature extremes: Effect on plant growth and development. Weather and Climate Extremes **10, Part A**, 4–10.

Hocking PJ, Meyer CP (Commonwealth S and IRO. 1991. Effects of CO2 enrichment and nitrogen stress on growth and partitioning of dry matter and nitrogen in wheat and maize. Australian Journal of Plant Physiology (Australia).

Hogan KP, Smith AP, Ziska LH. 1991. Potential effects of elevated CO2 and changes in temperature on tropical plants. Plant, Cell & Environment **14**, 763–778.

Högy P, Wieser H, Köhler P, Schwadorf K, Breuer J, Franzaring J, Muntifering R, Fangmeier A. 2009. Effects of elevated CO2 on grain yield and quality of wheat: results from a 3-year free-air CO2 enrichment experiment. Plant Biology **11**, 60–69.

Houshmandfar A, Fitzgerald GJ, O'Leary G, Tausz-Posch S, Fletcher A, Tausz M. 2017. The relationship between transpiration and nutrient uptake in wheat changes under elevated atmospheric CO2. Physiologia Plantarum **0**.

Hunsaker DJ, Kimball BA, Pinter PJ, LaMorte RL, Wall GW. 1996. Carbon dioxide enrichment and irrigation effects on wheat evapotranspiration and water use efficiency. Transactions of the ASAE (USA).

Jahan E, Thomson PC, Tissue DT. 2021. Mesophyll conductance in two cultivars of wheat grown in glacial to super-elevated CO2 concentrations. Journal of Experimental Botany **72**, 7191–7202.

Jauregui I, Aroca R, Garnica M, Zamarreño ÁM, García-Mina JM, Serret MD, Parry M, Irigoyen JJ, Aranjuelo I. 2015. Nitrogen assimilation and transpiration: key processes conditioning responsiveness of wheat to elevated [CO2] and temperature. Physiologia Plantarum **155**, 338–354.

Kimball BA. 1983. Carbon Dioxide and Agricultural Yield: An Assemblage and Analysis of 430 Prior Observations. Agronomy Journal **75**, 779–788.

Kimball BA. 2016. Crop responses to elevated CO2 and interactions with H2O, N, and temperature. Current Opinion in Plant Biology **31**, 36–43.

Kimball BA, LaMorte RL, Pinter PJ, Wall GW, Hunsaker DJ, Adamsen FJ, Leavitt SW, Thompson TL, Matthias AD, Brooks TJ. 1999. Free-air CO2 enrichment and soil nitrogen effects on energy balance and evapotranspiration of wheat. Water Resources Research **35**, 1179–1190.

Kimball BA, Pinter Jr. PJ, Garcia RL, La Morte RL, Wall GW, Hunsaker DJ, Wechsung G, Wechsung F, Kartschall T. 1995. Productivity and water use of wheat under free-air CO2 enrichment. Global Change Biology **1**, 429–442.

Krenzer EG, Moss DN. 1975. Carbon Dioxide Enrichment Effects Upon Yield and Yield Components in Wheat. Crop Science **15**, 71–74.

Lanigan GJ, Betson N, Griffiths H, Seibt U. 2008. Carbon Isotope Fractionation during Photorespiration and Carboxylation in Senecio. Plant Physiology **148**, 2013–2020.

Leakey ADB, Ainsworth EA, Bernacchi CJ, Rogers A, Long SP, Ort DR. 2009. Elevated CO2 effects on plant carbon, nitrogen, and water relations: six important lessons from FACE. Journal of Experimental Botany **60**, 2859–2876.

Liao M, Fillery IRP, Palta JA. 2004. Early vigorous growth is a major factor influencing nitrogen uptake in wheat. Functional Plant Biology **31**, 121–129.

Lobell DB, Gourdji SM. 2012. The Influence of Climate Change on Global Crop Productivity. Plant Physiology **160**, 1686–1697.

Long SP. 1991. Modification of the response of photosynthetic productivity to rising temperature by atmospheric CO2 concentrations: Has its importance been underestimated? Plant, Cell & Environment **14**, 729–739.

Long SP, Ainsworth EA, Leakey ADB, Nösberger J, Ort DR. 2006. Food for Thought: Lower-Than-Expected Crop Yield Stimulation with Rising CO2 Concentrations. Science **312**, 1918–1921.

Macabuhay AA. 2016. Physiological and biochemical responses of wheat to combined heat stress and elevated CO2 during grain-filling.

Macabuhay A, Houshmandfar A, Nuttall J, Fitzgerald GJ, Tausz M, Tausz-Posch S. 2018. Can elevated CO2 buffer the effects of heat waves on wheat in a dryland cropping system? Environmental and Experimental Botany **155**, 578–588.

Medlyn BE, Dreyer E, Ellsworth D, *et al.* 2002. Temperature response of parameters of a biochemically based model of photosynthesis. II. A review of experimental data. Plant, Cell & Environment **25**, 1167–1179.

Mishra D, Shekhar S, Chakraborty S, Chakraborty N. 2021. High temperature stress responses and wheat: impacts and alleviation strategies. Environmental and Experimental Botany, 104589.

Mitchell R a. C, Mitchell VJ, Driscoll SP, Franklin J, Lawlor DW. 1993. Effects of increased CO2 concentration and temperature on growth and yield of winter wheat at two levels of nitrogen application. Plant, Cell & Environment **16**, 521–529.

Morison JIL, Lawlor DW. 1999. Interactions between increasing CO2 concentration and temperature on plant growth. Plant, Cell & Environment **22**, 659–682.

Mosse J. 1990. Nitrogen-to-protein conversion factor for ten cereals and six legumes or oilseeds. A reappraisal of its definition and determination. Variation according to species and to seed protein content. Journal of Agricultural and Food Chemistry **38**, 18–24.

Mulholland BJ, Craigon J, Black CR, Colls JJ, Atherton J, Landon G. 1998. Growth, light interception and yield responses of spring wheat (Triticum aestivum L.) grown under elevated CO2 and O3 in open-top chambers. Global Change Biology **4**, 121–130.

Nie GY, Long SP, Garcia RL, Kimball BA, Lamorte RL, Pinter PJ, Wall GW, Webber AN. 1995. Effects of free-air CO2 enrichment on the development of the photosynthetic apparatus in wheat, as indicated by changes in leaf proteins. Plant, Cell & Environment **18**, 855–864.

Osborne CP, Roche JL, Garcia RL, Kimball BA, Wall GW, Pinter PJ, Morte RLL, Hendrey GR, Long SP. 1998. Does Leaf Position within a Canopy Affect Acclimation of Photosynthesis to Elevated CO2? Analysis of a Wheat Crop under Free-Air CO2Enrichment. Plant Physiology **117**, 1037–1045.

Perera RS, Cullen BR, Eckard RJ. 2019. Using Leaf Temperature to Improve Simulation of Heat and Drought Stresses in a Biophysical Model. Plants **9**, 8.

Pleijel H, Uddling J. 2012. Yield vs. Quality trade-offs for wheat in response to carbon dioxide and ozone. Global Change Biology **18**, 596–605.

Poorter H. 1993. Interspecific variation in the growth response of plants to an elevated ambient CO2 concentration. Vegetatio **104–105**, 77–97.

Poorter H, Navas M-L. 2003. Plant growth and competition at elevated CO2: on winners, losers and functional groups. The New Phytologist **157**, 175–198.

Porter JR, Gawith M. 1999. Temperatures and the growth and development of wheat: a review. European Journal of Agronomy **10**, 23–36.

Poudel PB. 2020. Heat Stress Effects and Tolerance in Wheat: A Review. , 6.

Prasad PVV, Pisipati SR, Ristic Z, Bukovnik U, Fritz AK. 2008. Impact of Nighttime Temperature on Physiology and Growth of Spring Wheat. Crop Science **48**, 2372–2380.

Rawson H. 1992. Plant Responses to Temperature Under Conditions of Elevated CO2. Australian Journal of Botany **40**, 473–490.

Rogers A, Humphries SW. 2000. A mechanistic evaluation of photosynthetic acclimation at elevated CO2. Global Change Biology **6**, 1005–1011.

Sadras V, Dreccer MF. 2015. Adaptation of wheat, barley, canola, field pea and chickpea to the thermal environments of Australia. Crop and Pasture Science **66**, 1137–1150.

Sage RF, Kubien DS. 2007. The temperature response of C3 and C4 photosynthesis. Plant, Cell & Environment **30**, 1086–1106.

Seneweera SP, Conroy JP. 1997. Growth, grain yield and quality of rice (Oryza sativa L.) in response to elevated CO2 and phosphorus nutrition. Soil Science and Plant Nutrition **43**, 1131–1136.

Sionit N, Mortensen DA, Strain BR, Hellmers H. 1981. Growth Response of Wheat to CO2 Enrichment and Different Levels of Mineral Nutrition. Agronomy Journal **73**, 1023–1027.

Stone P, Nicolas M. 1994. Wheat Cultivars Vary Widely in Their Responses of Grain Yield and Quality to Short Periods of Post-Anthesis Heat Stress. Functional Plant Biology **21**, 887–900.

Stone PJ, Nicolas M. 1996. Effect of Timing of Heat Stress During Grain Filling on Two Wheat Varieties Differing in Heat Tolerance. II. Fractional Protein Accumulation. Functional Plant Biology **23**, 739–749.

Stone PJ, Nicolas ME. 1998. The effect of duration of heat stress during grain filling on two wheat varieties differing in heat tolerance: grain growth and fractional protein accumulation. Functional Plant Biology **25**, 13–20.

Taub DR, Miller B, Allen H. 2008. Effects of elevated CO2 on the protein concentration of food crops: a meta-analysis. Global Change Biology **14**, 565–575.

Taub DR, Wang X. 2008. Why are nitrogen concentrations in plant tissues lower under elevated CO2? A critical examination of the hypotheses. Journal of Integrative Plant Biology **50**, 1365–1374.

Tausz M, Norton RM, Tausz-Posch S, Löw M, Seneweera S, O'Leary G, Armstrong R, Fitzgerald GJ. 2017. Can additional N fertiliser ameliorate the elevated CO2-induced depression in grain and tissue N concentrations of wheat on a high soil N background? Journal of Agronomy and Crop Science **203**, 574–583.

Tausz-Posch S, Dempsey RW, Seneweera S, Norton RM, Fitzgerald G, Tausz M. 2015. Does a freely tillering wheat cultivar benefit more from elevated CO2 than a restricted tillering cultivar in a water-limited environment? European Journal of Agronomy **64**, 21–28.

Tcherkez G, Ben Mariem S, Larraya L, *et al.* 2020. Elevated CO2 has concurrent effects on leaf and grain metabolism but minimal effects on yield in wheat. Journal of Experimental Botany **71**, 5990–6003.

Von Caemmerer S, Evans JR. 2015. Temperature responses of mesophyll conductance differ greatly between species. Plant, Cell & Environment **38**, 629–637.

Wahid A, Gelani S, Ashraf M, Foolad MR. 2007. Heat tolerance in plants: An overview. Environmental and Experimental Botany **61**, 199–223.

Wang D, Heckathorn SA, Barua D, Joshi P, Hamilton EW, LaCroix JJ. 2008. Effects of elevated CO2 on the tolerance of photosynthesis to acute heat stress in C3, C4, and CAM species. American Journal of Botany **95**, 165–176.

Wang D, Heckathorn SA, Wang X, Philpott SM. 2011. A meta-analysis of plant physiological and growth responses to temperature and elevated CO2. Oecologia **169**, 1–13.

Wang X, Liu F. 2021. Effects of Elevated CO2 and Heat on Wheat Grain Quality. Plants **10**, 1027.

Wang X, Liu F, Jiang D. 2017. Priming: A promising strategy for crop production in response to future climate. Journal of Integrative Agriculture **16**, 2709–2716.

Wardlaw IF, Blumenthal C, Larroque O, Wrigley CW. 2002. Contrasting effects of chronic heat stress and heat shock on kernel weight and flour quality in wheat. Functional Plant Biology **29**, 25–34.

Wardlaw IF, Moncur L. 1995. The Response of Wheat to High Temperature Following Anthesis. I. The Rate and Duration of Kernel Filling. Functional Plant Biology **22**, 391–397.

Welch JR, Vincent JR, Auffhammer M, Moya PF, Dobermann A, Dawe D. 2010. Rice yields in tropical/subtropical Asia exhibit large but opposing sensitivities to minimum and maximum temperatures. Proceedings of the National Academy of Sciences **107**, 14562–14567.

Yin X, Struik PC. 2009. C3 and C4 photosynthesis models: An overview from the perspective of crop modelling. NJAS - Wageningen Journal of Life Sciences **57**, 27–38.

Zadoks JC, Chang TT, Konzak CF. 1974. A decimal code for the growth stages of cereals. Weed Research **14**, 415–421.

Zhang X, Högy P, Wu X, Schmid I, Wang X, Schulze WX, Jiang D, Fangmeier A. 2018. Physiological and Proteomic Evidence for the Interactive Effects of Post-Anthesis Heat Stress and Elevated CO2 on Wheat. PROTEOMICS **18**, 1800262.

Zhang H, Turner NC, Simpson N, Poole ML. 2010. Growing-season rainfall, ear number and the water-limited potential yield of wheat in south-western Australia. Crop and Pasture Science **61**, 296–303.

Ziska LH, Morris CF, Goins EW. 2004. Quantitative and qualitative evaluation of selected wheat varieties released since 1903 to increasing atmospheric carbon dioxide: can yield sensitivity to carbon dioxide be a factor in wheat performance? Global Change Biology **10**, 1810–1819.

Table 1 Summary of modelled parameters for temperature response of photosynthesis. Summary of coefficients derived using nonlinear least square fitting of CO_2 assimilation rates and maximal rate of carboxylation (V_{cmax}) and maximal rate of RuBP regeneration (J_{max}) determined using A-C_i response curves and dark respiration measured at five leaf temperatures 15, 20, 25, 30 and 35°C. Values are means with standard errors. Derived parameters include temperature optima (T_{opt}) of photosynthesis (A_{opt}); activation energy for carboxylation (EaV); activation energy (EaJ), entropy term (ΔSJ) and T_{opt} and corresponding value for J_{max} with deactivation energy (Hd) assumed constant; and activation energy (EaR) and temperature coefficient (Q_{10}) for dark respiration. Letters indicate significance of variation in means.

Parameter	Constant	Scout	Yitpi
A_{sat} (µmol m^{-2} s^{-1})	T_{opt} (°C)	23.4 ± 1 a	23.4 ± 0.7 a
	A_{opt}	24.6 ± 1 a	22 ± 0.6 b
g_m (mol m^{-2} s^{-1} bar^{-1})	T_{opt} (°C)	27.9 ± 2.2 a	32.5 ± 6.9 b
	g_m at 25°C	0.31 ± 0.01 a	0.25 ± 0.01 b
	g_m at T_{opt}	0.30 ± 0.01	0.25 ± 0.01
V_{cmax} (µmol m^{-2} s^{-1})	V_{cmax} at 25°C	192.7 ± 17.1 a	198.4 ± 17.7 a
	EaV (kJ mol^{-1})	43.3 ± 8.74 a	46.4 ± 8.7 a
J_{max} (µmol m^{-2} s^{-1})	J_{max} at 25°C	187.9 ± 13.1 a	186.1 ± 5.7 a
	T_{opt} (°C)	29.6 ± 0.3 a	30.5 ± 0.3 a
	J_{max} at T_{opt}	205.7 ± 10.2	215.4 ± 13.4
	EaJ (kJ mol^{-1})	37.7 ± 13.2 a	41.1 ± 5.8 a
	ΔSJ (J mol^{-1} K^{-1})	648.3 ± 5.3 a	647 ± 2.4 a
	Hd (kJ mol^{-1})	200	
Rd (µmol m^{-2} s^{-1})	*Rd* at 25°C	1.25 ± 0.02 a	1.25 ± 0.02 a
	EaR (kJ mol^{-1})	30.9 ± 1.6 a	33.2 ± 1.7 a
	Q_{10}	1.51 ± 0.03 a	1.56 ± 0.04 a

680

Figure Legends

Figure 1 Temperature response of photosynthetic parameters: CO_2 assimilation rate (a), mesophyll conductance (b), stomatal conductance (c) and intercellular CO_2 (d), V_{cmax} (e), J_{max} (f), J_{max} / V_{cmax} (g) and dark respiration (h) over leaf temperatures (15, 20, 25, 30 and 35 °C) in plants grown at aCO_2. Scout and Yitpi are depicted using circles with solid cultivars and triangles with broken cultivars respectively. Data in panels (a), (b), (c), (d), (e), (f) and (h) are fit using nonlinear least square (nls) function in R.

Figure 2 Response of leaf gas exchange parameters to eCO_2 under non-HS conditions. Measurements were made at 25°C before each harvest (T1, T2 and T3) for CO_2 assimilation rates (a, b) and stomatal conductance (c, d) in Scout (Circles) and Yitpi (Triangles). Plants were grown and measured at aCO_2 (blue solid cultivars), grown and measured at eCO_2 (red solid cultivars), and grown at eCO_2 and measured at 400 µL CO_2 L^{-1} (red dashed cultivars). Statistical significance levels (t-test) for the growth condition within each cultivar are shown and they are: * = p < 0.05; ** = p < 0.01: *** = p < 0.001.

Figure 3 Response of photosynthesis and chlorophyll fluorescence to HS in Scout and Yitpi grown at aCO_2 or eCO_2. CO_2 assimilation rates (a, b, c, d) and dark-adapted chlorophyll fluorescence, Fv/Fm (e, f, g, h) were measured at growth CO_2 and 25 °C in Scout (Circles) and Yitpi (Triangles)**.** Open and closed symbols represent control and HS plants, respectively. In addition, plants were measured at 35°C (*) during both HS cycles.

Figure 4 Response of photosynthetic parameters to eCO_2 and HS at anthesis (T3) in Scout and Yitpi. CO_2 assimilation rate (a, b), stomatal conductance (c, d), photosynthetic water use efficiency (e, f) and photosynthetic nitrogen use efficiency (g, h) were measured at growth CO_2. V_{cmax} (i, j) and J_{max} (k, l) were derived from ACi curves measured at 25^{o}C. Cultivars indicate means and shaded region is 95% confidence interval. Data shown for control (not exposed to any heat stress) and plants exposed to both heat stress cycles (HS1+2). Statistical significance levels (t-test) for the growth condition within each cultivar are shown and they are: * = p < 0.05; ** = p < 0.01: *** = p < 0.001.

Figure 5 Relationships with leaf gas exchange and grain yield across treatments. CO_2 assimilation rate plotted as a function of stomatal conductance (a) (both aCO_2 and eCO_2 grown plants measured at 400 µl L^{-1}), J_{max} plotted as a function of V_{cmax} (b) and grain protein plotted as a function of yield (c) in Scout

(Circles) and Yitpi (Triangles). Ambient and elevated CO_2 are depicted in blue and red, respectively. Control and heat stressed plants depicted using open and closed symbols. Panel a depicts data for control, HS1, HS2 and both heat stresses (HS1+2), while panels b and cinclude only control and HS1+2.

Figure 6 Response of plant growth and morphological traits to elevated CO_2 and HS: Total dry mass (a, b), tillers or number of tillers (c, d), leaf area (e, f), leaf number (g, h) and height (i, j) were measured at different time points across the life cycle of wheat cultivars Scout (Circles) and Yitpi (Triangles). Ambient and elevated CO_2 are depicted in blue and red color, respectively. Open symbols connected with solid cultivars and closed symbols connected with dashed cultivars represent control and HS plants, respectively. HS1 and HS2 depict the timing of HS applied at 10 and 15 weeks after planting respectively.

Figure 7 Response of total plant dry mass and grain parameters to growth at eCO_2 and HS at maturity (T4): Total dry mass (a, b), grain dry mass (c, d), grain number (e, f) and grain nitrogen (g, h) were measured at the final harvest. Cultivars indicate means and shaded region is 95% confidence interval. Ambient and elevated CO_2 are depicted in blue and red color respectively. Heat stress levels include plants not exposed to any heat stress (control) and both heat stresses (HS1+2). Statistical significance levels (t-test) for the growth condition within each cultivar is shown and they are: * = $p < 0.05$; ** = $p < 0.01$: *** = $p < 0.001$.

Supplementary Materials

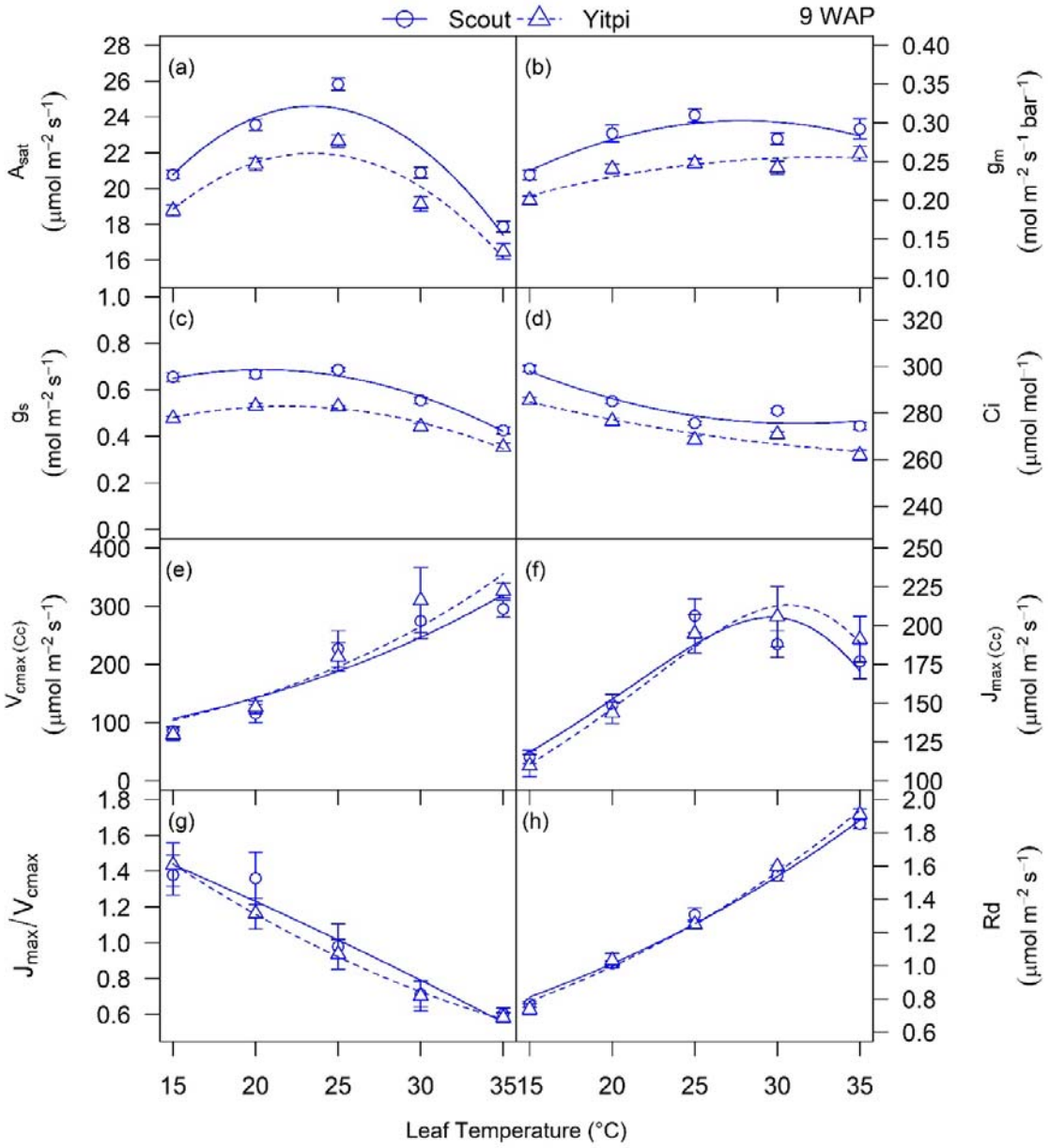

Figure 1 Temperature response of photosynthetic parameters: CO_2 assimilation rate (a), mesophyll conductance (b), stomatal conductance (c) and intercellular CO_2 (d), V_{cmax} (e), J_{max} (f), J_{max} / V_{cmax} (g) and dark respiration (h) over leaf temperatures (15, 20, 25, 30 and 35 °C) in plants grown at aCO_2. Scout and Yitpi are depicted using circles with solid cultivars and triangles with broken cultivars respectively. Data in panels (a), (b), (c), (d), (e), (f) and (h) are fit using nonlinear least square (nls) function in R.

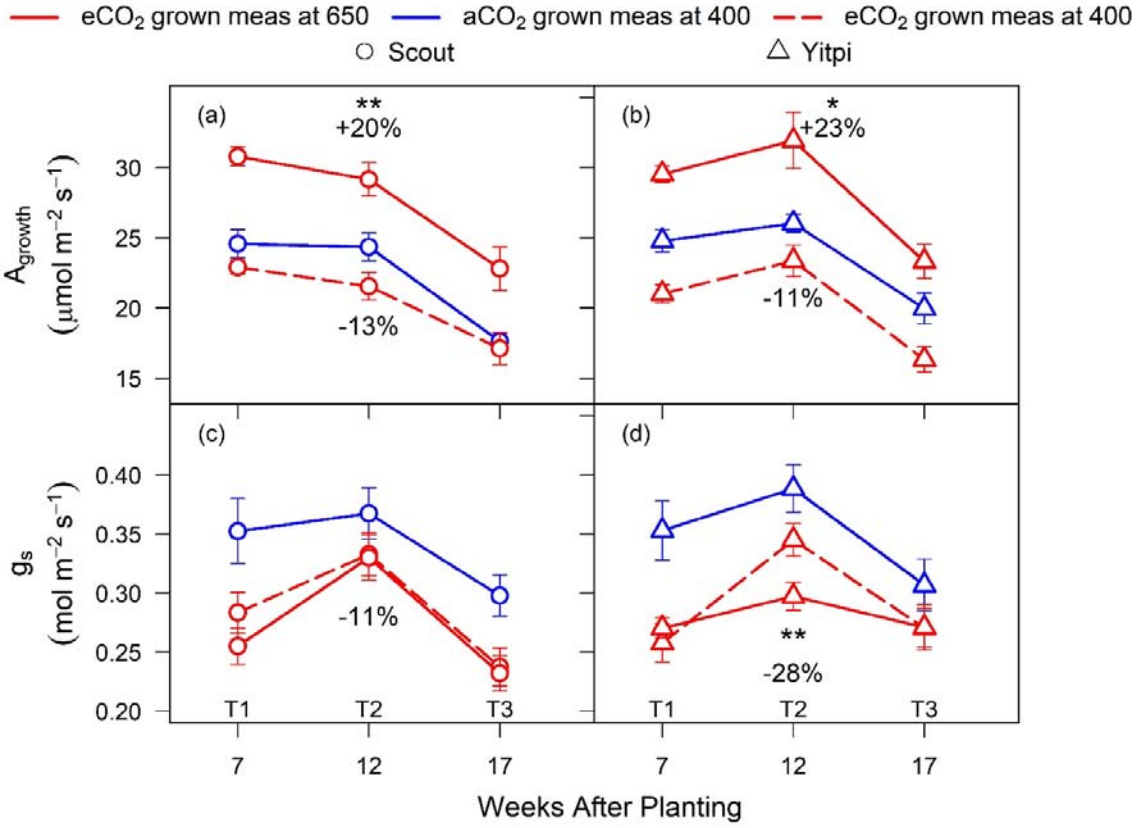

Figure 2 Response of leaf gas exchange parameters to eCO_2 under non-HS conditions. Measurements were made at 25°C before each harvest (T1, T2 and T3) for CO_2 assimilation rates (a, b) and stomatal conductance (c, d) in Scout (Circles) and Yitpi (Triangles). Plants were grown and measured at aCO_2 (blue solid cultivars), grown and measured at eCO_2 (red solid cultivars), and grown at eCO_2 and measured at 400 µL CO_2 L^{-1} (red dashed cultivars). Statistical significance levels (t-test) for the growth condition within each cultivar are shown and they are: * = p < 0.05; ** = p < 0.01: *** = p < 0.001.

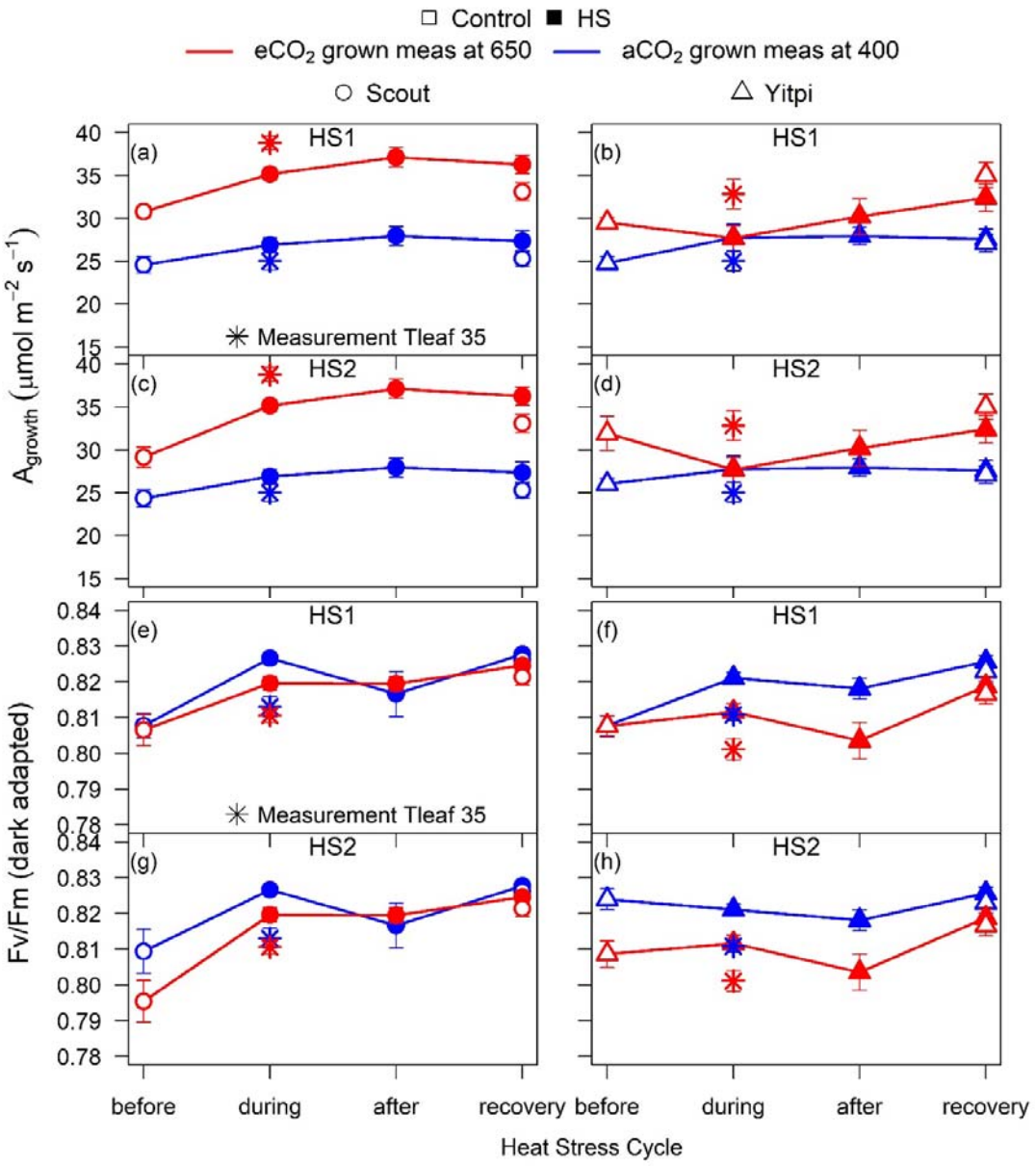

Figure 3 Response of photosynthesis and chlorophyll fluorescence to HS in Scout and Yitpi grown at aCO_2 or eCO_2. CO_2 assimilation rates (a, b, c, d) and dark-adapted chlorophyll fluorescence, Fv/Fm (e, f, g, h) were measured at growth CO_2 and 25 °C in Scout (Circles) and Yitpi (Triangles)**.** Open and closed symbols represent control and HS plants, respectively. In addition, plants were measured at 35°C (*) during both HS cycles.

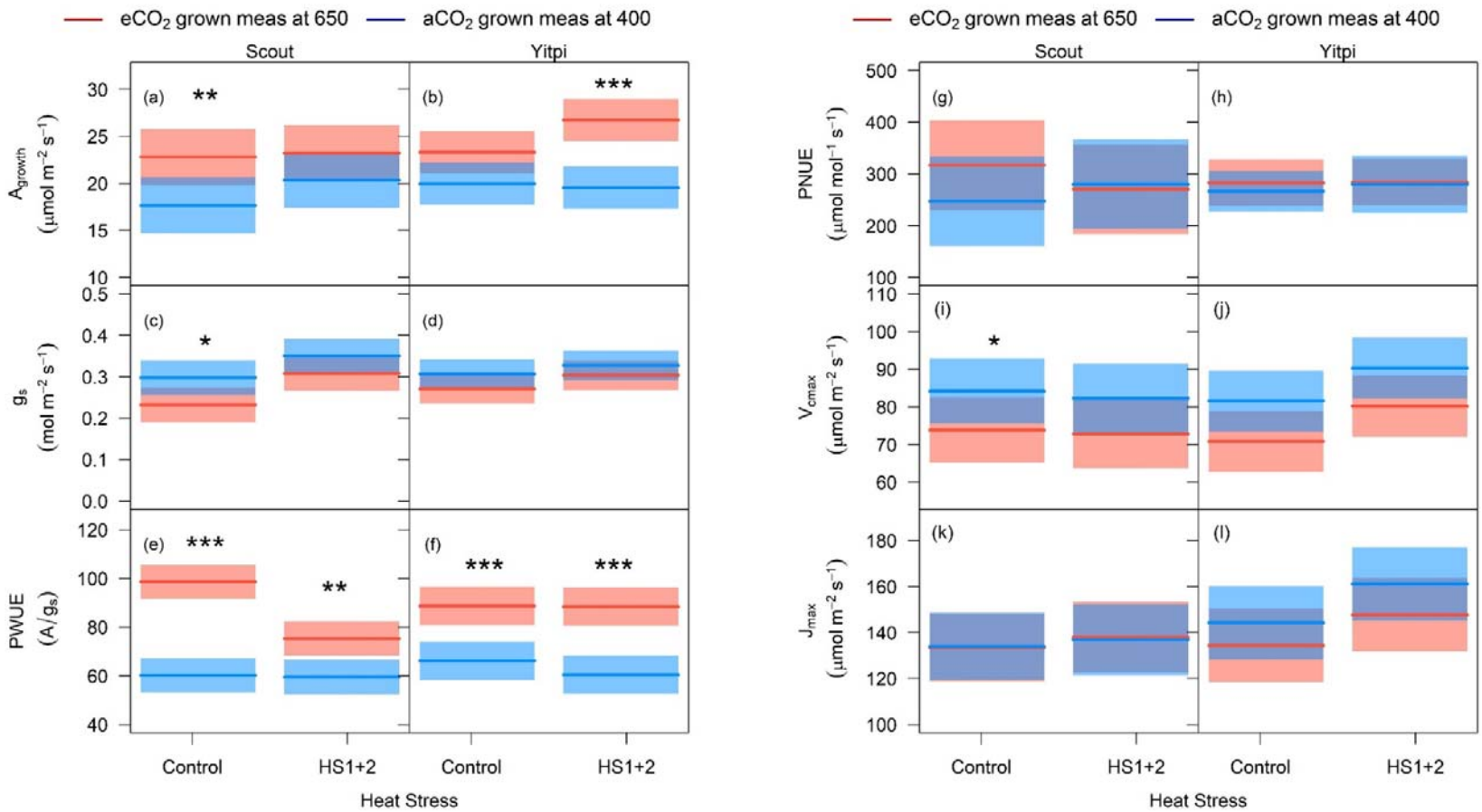

Figure 4 Response of photosynthetic parameters to eCO_2 and HS at anthesis (T3) in Scout and Yitpi. CO_2 assimilation rate (a, b), stomatal conductance (c, d), photosynthetic water use efficiency (e, f) and photosynthetic nitrogen use efficiency (g, h) were measured at growth CO_2. V_{cmax} (i, j) and J_{max} (k, l) were derived from ACi curves measured at 25°C. Cultivars indicate means and shaded region is 95% confidence interval. Data shown for control (not exposed to any heat stress) and plants exposed to both heat stress cycles (HS1+2). Statistical significance levels (t-test) for the growth condition within each cultivar are shown and they are: * = $p < 0.05$; ** = $p < 0.01$: *** = $p < 0.001$.

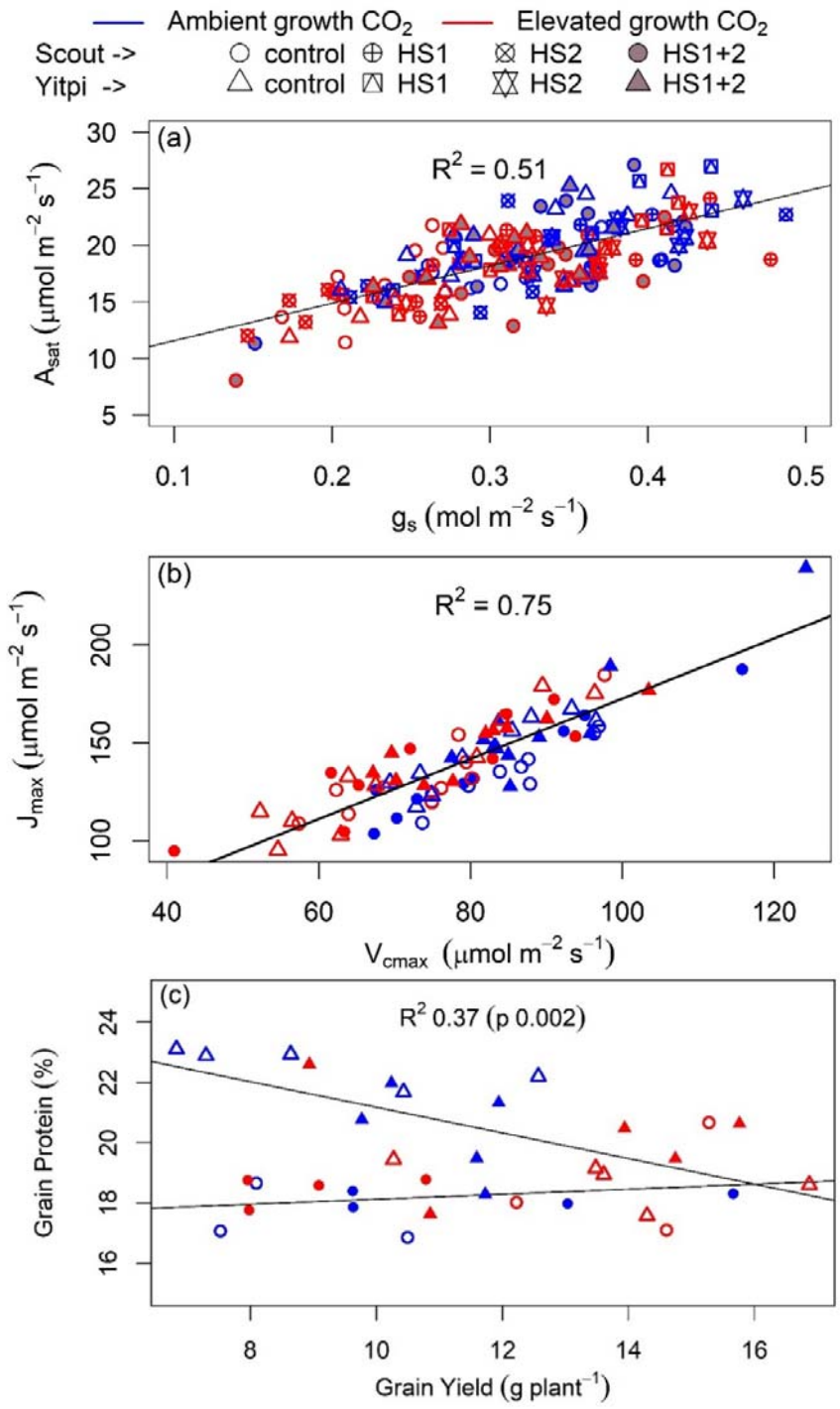

Figure 5 Relationships with leaf gas exchange and grain yield across treatments. CO_2 assimilation rate plotted as a function of stomatal conductance (a) (both aCO_2 and eCO_2 grown plants measured at 400 µl L^{-1}), J_{max} plotted as a function of V_{cmax} (b) and grain protein plotted as a function of yield (c) in Scout (Circles) and Yitpi (Triangles). Ambient and elevated CO_2 are depicted in blue and red, respectively. Control and heat stressed plants depicted using open and closed symbols. Panel a depicts data for control, HS1, HS2 and both heat stresses (HS1+2), while panels b and cinclude only control and HS1+2.

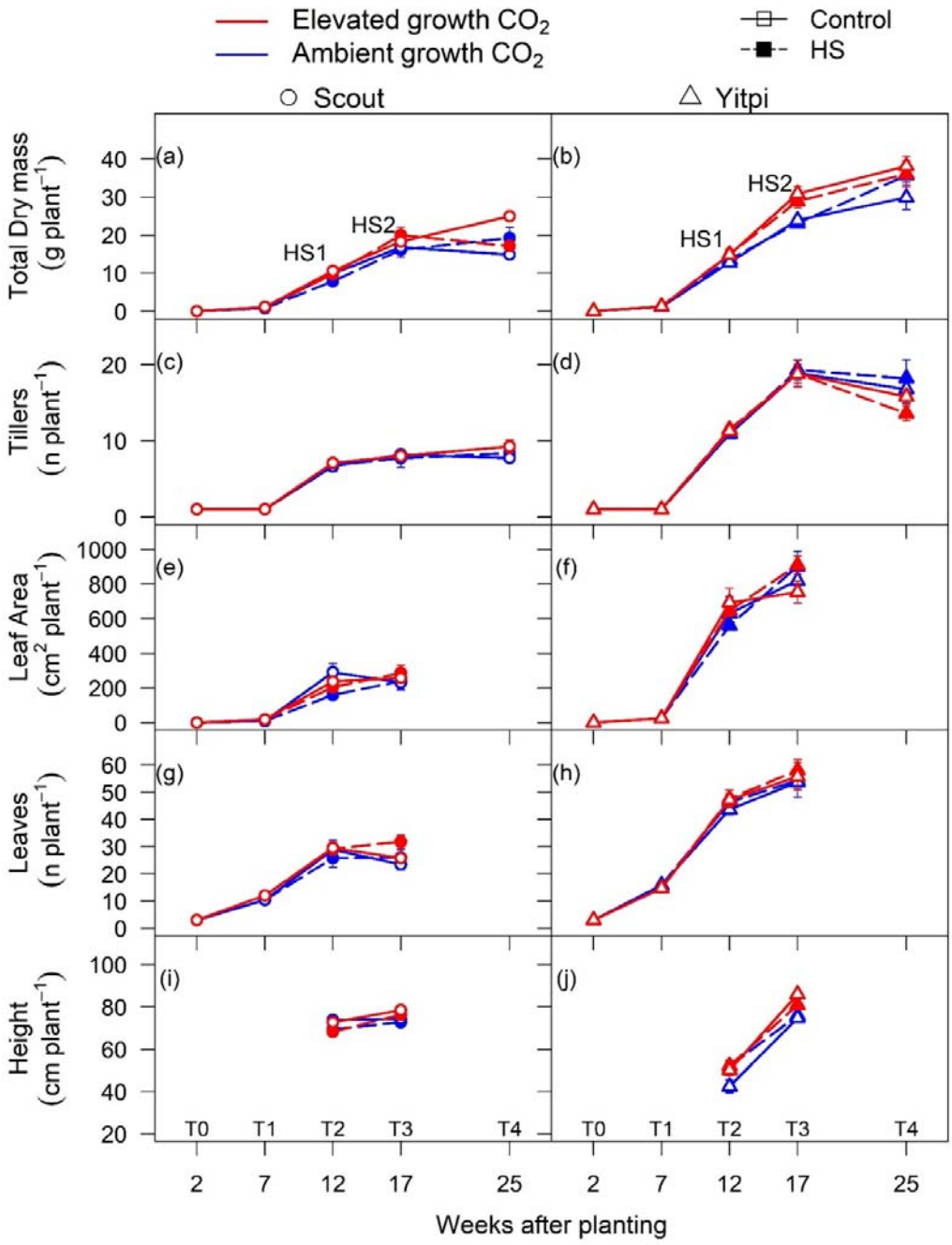

Figure 6 Response of plant growth and morphological traits to elevated CO_2 and HS: Total dry mass (a, b), tillers or number of tillers (c, d), leaf area (e, f), leaf number (g, h) and height (i, j) were measured at different time points across the life cycle of wheat cultivars Scout (Circles) and Yitpi (Triangles). Ambient and elevated CO_2 are depicted in blue and red color, respectively. Open symbols connected with solid cultivars and closed symbols connected with dashed cultivars represent control and HS plants, respectively. HS1 and HS2 depict the timing of HS applied at 10 and 15 weeks after planting respectively.

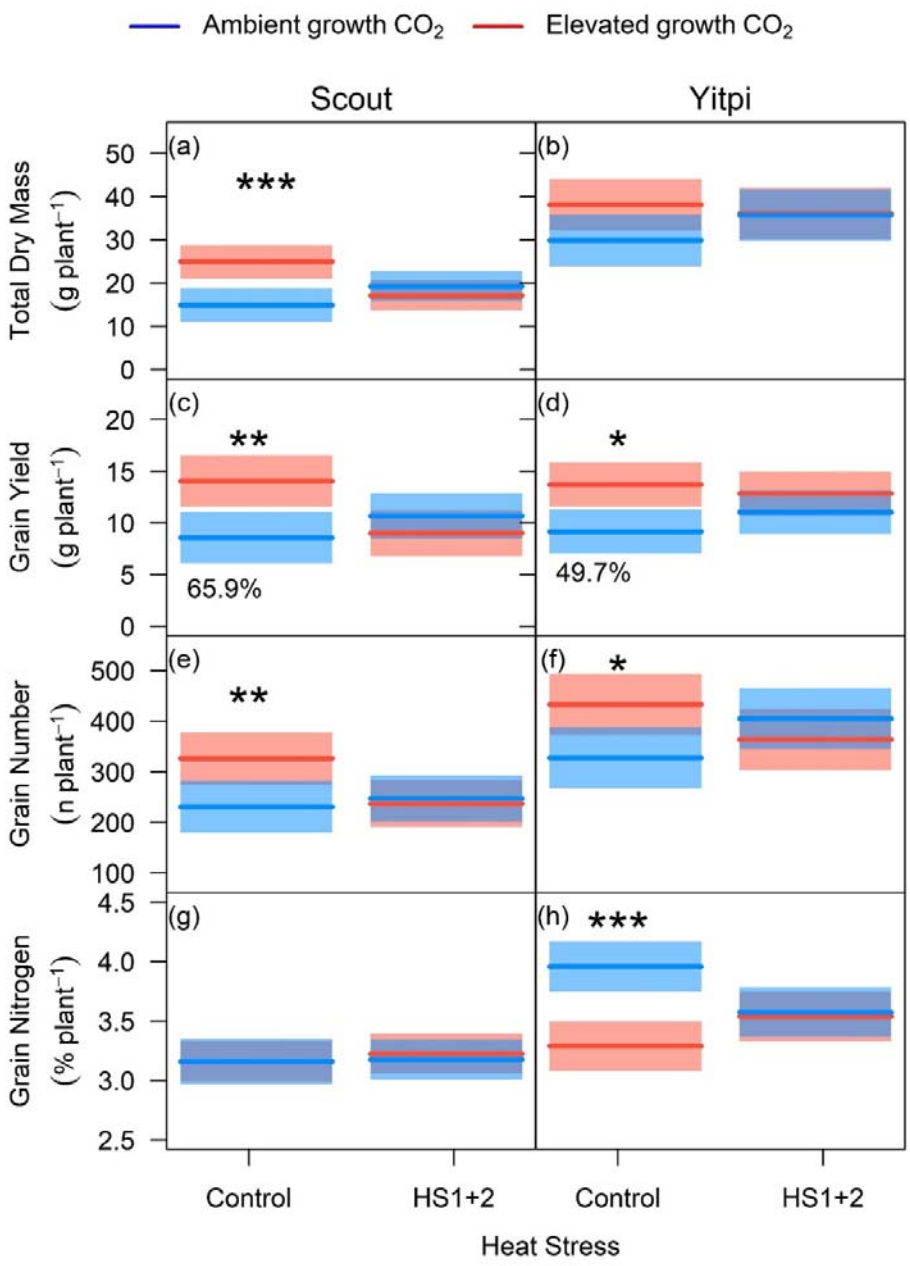

Figure 7 Response of total plant dry mass and grain parameters to growth at eCO_2 and HS at maturity (T4): Total dry mass (a, b), grain dry mass (c, d), grain number (e, f) and grain nitrogen (g, h) were measured at the final harvest. Cultivars indicate means and shaded region is 95% confidence interval. Ambient and elevated CO_2 are depicted in blue and red color respectively. Heat stress levels include plants not exposed to any heat stress (control) and both heat stresses (HS1+2). Statistical significance levels (t-test) for the growth condition within each cultivar is shown and they are: * = $p < 0.05$; ** = $p < 0.01$: *** = $p < 0.001$.